

# Exoplanets in extreme environments: auroras on pulsar planets

Miljenko Čemeljić

&

Sergio Joya

Physikalisches Institut, University of Bern

&

Nicolaus Copernicus Superior School, College of  
Astronomy and Natural Sciences, Torun, Poland

&

Nicolaus Copernicus Astronomical Center of the  
Polish Academy of Sciences, Warsaw, Poland

&

Institute of Physics, Silesian University in Opava,  
Czech Republic

&

Academia Sinica Institute of Astronomy and  
Astrophysics, Taipei, Taiwan

with Tanja Kaister, Piyush Marmat, Marco Velli,  
Jacobo Varela



- Introduction: planets around pulsars
- Aurora in Solar System and exoplanets
- Simulations of star-planet magnetosphere interaction
- Radio emission from aurora on planets around pulsars
- Art preceding Science
- Alfven waves in super-relativistic pulsar wind -Sergio's part
- Summary

- Exoplanets were long anticipated, but nobody expected it around a pulsar! **The first exoplanets** were found in orbit around a Galactic disk 6.2-ms pulsar PSR1257+12 (**Wolszczan & Frail, 1992**). *Actually, probably it is not so unexpected that a Polish scientist found it: Demianski & Proszynski (1979) discussed such a possibility for a planet around PSR B0329+54, 3 460 ly away in Camelopardalis, period 0.71452 s, 5 million yrs old. Because of non-detection by others it was rejected, but as of today the possibility of a long period planet is still not refuted.*
- The first planet around a “normal” star was found in 1995, in a decades long search by Mayor & Queloz (not a chance discovery as Wolszczan’s) and was awarded with a Nobel prize in 2019. It was the first “hot Jupiter”, a large gaseous planet (named in NameExoWorlds as Dimidium=“half” in Latin, because of half Jupiter mass) with a surprising period of 4.2 days, orbiting very closely the star 51 Pegasi.
- The precise timing is essential: Wolszczan’s pulsar rotates about its axis 161 times per second, period  $P = 6.219 \times 10^{-3}$  s and a period derivative of  $\dot{P} = 1.2 \times 10^{-19}$ . In a standard magnetic dipole spindown model  $B = 3 \times 10^{19} (P\dot{P})^{(1/2)} \text{ G} \approx 8.8 \times 10^8 \text{ G}$  and a characteristic age  $\tau = P/(2 \dot{P}) = 8 \times 10^8 \text{ yrs}$ . It is the fastest moving pulsar, with transverse velocity 326 km/s and its surface is hot, 29 000 K, 2300 ly (710 pc) from us, in the constellation Virgo. Planets A,B,C masses 0.02 (2  $M_{\text{Moon}}$ ), 4.3 and 3.9 Earth masses, at 0.19, 0.36 and 0.46 AU from pulsar, in almost circular orbits at inclinations 50, 53, 47 degrees, periods of 25.3, 66.6 and 98 days. The fourth possible planet in this system (Wolszczan 1996) was later dismissed (Wolszczan et al. 2000a).
- In 2015, in NameExoWorlds campaign, pulsar, which is an undead star, got the name of a Lich, undead character from fantasy fiction, known for controlling other undead creatures with magic. Planets are named Draugr, Poltergeist and Phobetor for planets A, B and C, respectively, by Norse mythology undead, noisy ghosts of supernatural world, and a character from Ovid's Metamorphoses (one of the thousand sons of Somnus=Sleep who appears in dreams in the form of beasts).

## Formation of planets around pulsars

Pulsars are formed when an old star uses all the fuel. It first implodes, then explodes, and finally settles into the neutron star. Very violent processes, not only for star, but also its environment. Nobody really expected planets around pulsars.

The formation mechanisms of planets around pulsars can be divided into presupernova and postsupernova scenarios:

- **Presupernova** scenario includes formation of planets around an ordinary star and either surviving the evolution (and a series of catastrophic events along it) or being captured by a NS.
- In **postsupernova** cases, planets are either formed from the material around newly formed NS (the **second generation planets**), or they are the last stage in the formation of some binary millisecond pulsars.
- For the rocky planets in circular orbits, a good possibility are mergers like WD+WD or WD+NS, or the remnant disk of the material from a Be star forming a binary with a NS. Wolszczan's planets best match the WD-WD merger scenario, so that planets are formed out of the debris of a merged companion star that used to orbit the pulsar when it was a white dwarf.
- Planets around pulsars seem to be rare, there are only few cases in about 3000 pulsars, 0.5%, all found by pulsar timing variations. Of more than 5000 currently known exoplanets, less than 10 around pulsars are confirmed.

-Wolszczan & Frail (1992) PSR1257+12, A,B,C

(1993) PSR B1620–26 A + WD with one exoplanet ( $2.5 \pm 1 M_{\text{Jupiter}}$ , orbiting them at 23 AU, period 36500 days~10 yrs, found from Doppler shifts it induced on the orbits of stars). It is in Scorpius, at a distance 12.4ly away, just outside the core of the globular cluster M4 which is 12.2 bln years old. Stars are hot:  $<30\,000\text{ K}$  and  $<25\,200\text{ K}$ . It is most probably a captured planet.

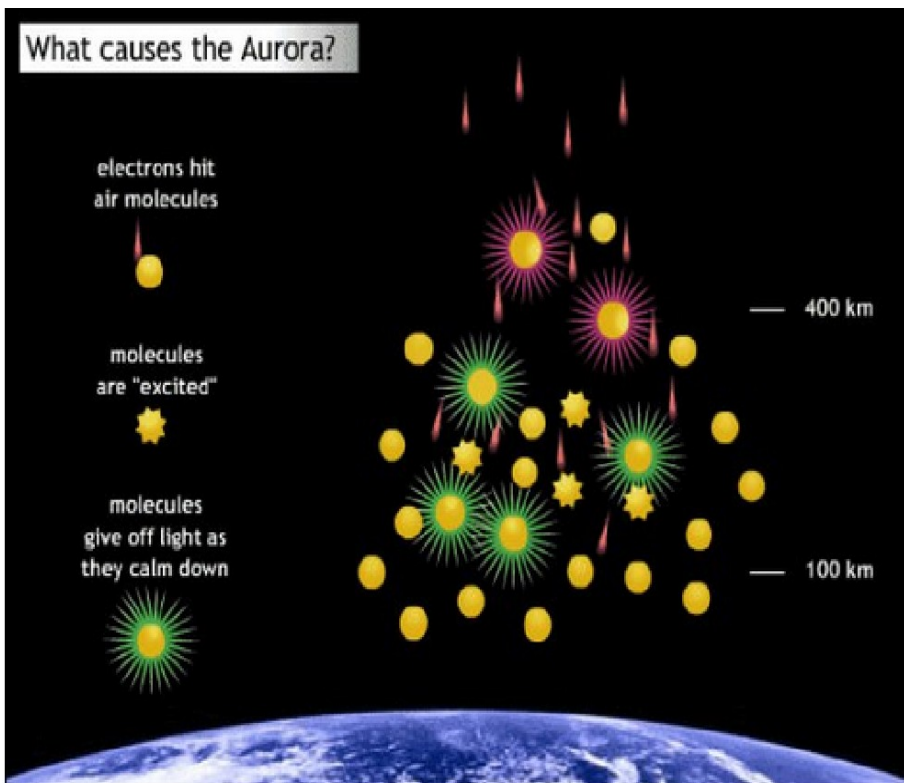
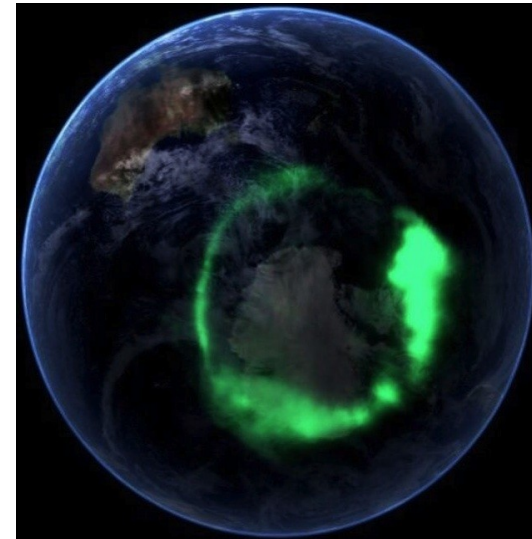
-(2006) 4U 0142+61, a magnetar (supernova about 100 000 yrs ago, 0.63 solar luminosities, rotates with 8.7s period) in Cassiopeia, at 13 000 ly from us, debris disk detected, at 1.6 mln km from the star, contains about 10 Earth masses of material, mostly heavier metals.

-(2011) The “diamond-planet” system PSR J1719–1438 is a millisecond pulsar surrounded by a Jupiter-mass companion at least 23 times denser than water, thought to have formed via ablation (evaporation) of its donor star. It is a 27 000km radius  $10^{31}$  carats diamond crystal core remaining from the evaporated white dwarf, at 600 000 km from the star, has 2hr10’ rotation period. – of the similar kind is a Black Widow pulsar PSR B1957+20 (1988) in Sagitta constellation, with a period of 1.6ms and large mass, 1.6-2.4  $M_{\text{Sun}}$ . It has a  $\sim M_{\text{Jupiter}}$  companion, probably a brown dwarf, orbiting it with a period of 9.2hrs, making a 20min eclipses, through which the object was found.

-(1968 pulsar, 2013 asteroid?) PSR J0738–4042, encounter with an asteroid or in-falling debris from a disk. It is a bright, radio-emitting neutron star at a distance 37 000 ly in constellation Puppis, with rotational properties similar to the main population of middle aged, isolated, radio pulsars, P and  $\dot{P}$  0.267 1/s (375ms) and  $-1/15e^{-14} 1/s^2$ , collected 24 yrs of data, so one can check the timing in detail.

-(1968 Puschino pulsar, 2014 planets) PSR B0943+10 is an 5mln years old pulsar in Leo, 2 000 ly away, with period 1.1s. Two gas giant planets, masses 2.8 and 2.6  $M_{\text{Jup}}$  with 730 and 1460 days orbital period, 1/8 and 2.9 AU radius orbits, respectively. There are more tentative objects with planets of Jupiter mass, like low luminosity (2017) PSR J2322–2650, with planet of 0.8  $M_{\text{Jup}}$  in the orbit with 0.32d at 0.01 AU; (2022) PSR J2007-3120 with a 0.008  $M_{\text{J}}$  planet with 723d period; (2020, FAST) confirmed in globular cluster M13, PSR J1641+3627F, 3ms pulsar with a 0.16  $M_{\text{Sun}}$  mass companion, probably a WD, not a planet; the binary millisecond pulsar (2021, FAST) PSR J1641+3627E (also M13E) is a black widow with a companion mass around 19.42  $M_{\text{J}}$ , 0.11d period; (2013) PSR J1544+493 eclipsing black widow 2.16 ms pulsar with a close companion of 18  $M_{\text{Jup}}$  at 2.19h orbit; (2016) PSR J0636+5129 with a 8  $M_{\text{J}}$  companion in 96min orbit; (1996, 2001?) PSR J2051–0827, 28.3  $M_{\text{Jup}}$  at 0.1d period orbit, (2000) PSR J1807-2459, 9.4  $M_{\text{J}}$ , 0.07days period.





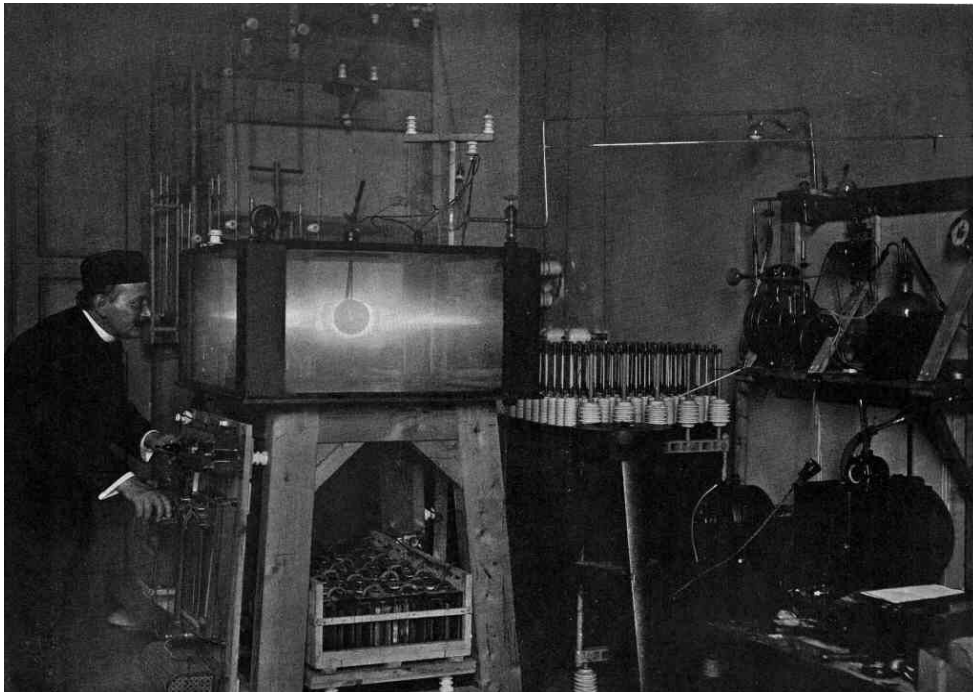
*High-speed particles from the Sun, mostly electrons, strike oxygen and nitrogen atoms in Earth's upper atmosphere. Credit: NASA*

Aurora, named **aurora borealis** (the Greek goddess of dawn, Aurora, + Greek name for northern wind, Boreas) was scientifically discussed by Pierre Gassendi in 1621.

It is an outcome of star-planet magnetospheric interaction. On Earth, aurora is visible close to the geographic poles, since they are also currently close to the magnetic poles of Earth. Aurora appears at  $>100$ -500 km, well above the von Karman line at 80-100 km, where airplanes are not supported by the air pressure any more, while ionosphere is from 50-1000 km.

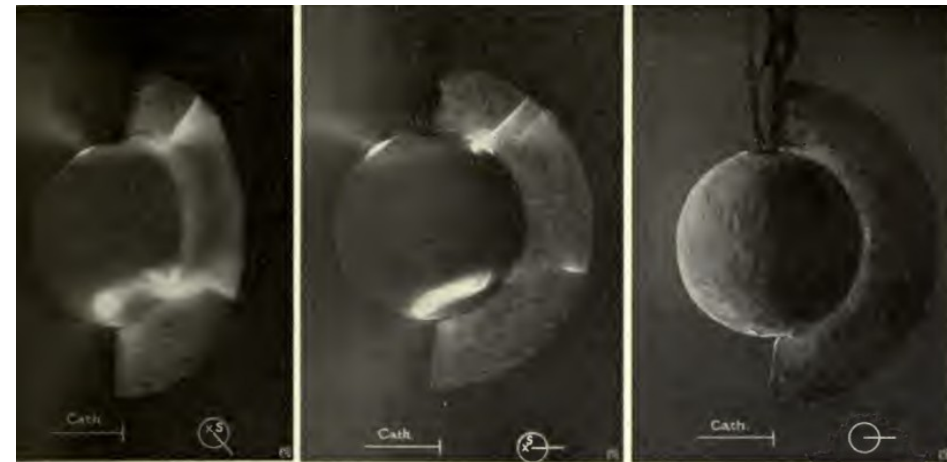
Colors in aurora come from different gases in the upper layers of the atmosphere emitting light of different colors in collision with particles from the solar wind (mostly electrons in this case). Oxygen emits greenish or brown-red, and nitrogen blue or red light.

# Aurora on Earth-Kristian Birkeland



Kristian Birkeland (1867 Oslo-1917 Tokyo) made electric models of **terrella** and measured magnetic fields and currents on continental scale. He funded his experiments by finding the use of powerful electric arcs in the fertilizer and aluminum production industry-it led to the large enrichment of whole Norway!

At the beginning of XX ct. he correctly explained the mechanism of aurora, but his results were for long time ridiculed (e.g. by Sydney Chapman, 1888-1970, later a leading researcher on geomagnetism)-they were accepted only after **1963**. when confirmed by cosmic probes.



a. b. c.

Fig. 46.

a horizontal current for a long distance between Dyrafjord and Axeloen. This would satisfactorily explain the constant direction that the perturbation in this and other similar cases shows.

In order to obtain a clear conception of the conditions, we will once more have recourse to my experiments with the terrella. The experiments shown in fig. 46, *a*, *b* and *c*, follow directly on to those in fig. 38, *a*, *b* and *c*. In fig. 46 *a*, the terrella is so turned that the screen forms an angle of  $135^\circ$  with its first position (fig. 38 *a*). In the next experiment (fig. 46 *b*), the angle is  $180^\circ$ . The angles are here measured from west to east. Fig. 46 *c* shows how the cathode rays strike the terrella; when the latter is not magnetic, but is in the same position as in the experiment given in fig. 46 *b*, only the half that is turned towards the cathode becomes luminous with phosphorescence.

It will be seen from figs. 46 *a* & *b* how the cathode rays behave when the terrella is very powerfully magnetised.

We will here especially direct our attention to the luminous wedge that is thrown upon the screen at about the 70th parallel

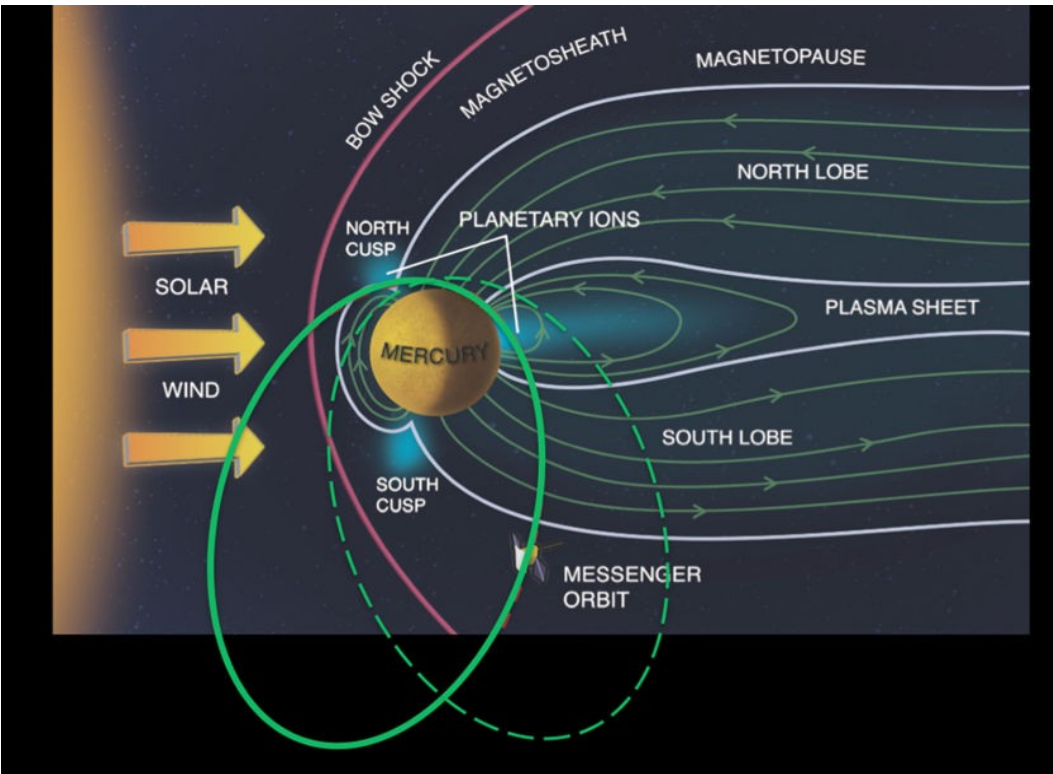


He might be the first to predict a plasma-filled space in **1913**, writing: "It seems to be a natural consequence of our points of view to assume that **the whole of space is filled with electrons and flying electric ions of all kinds...**"

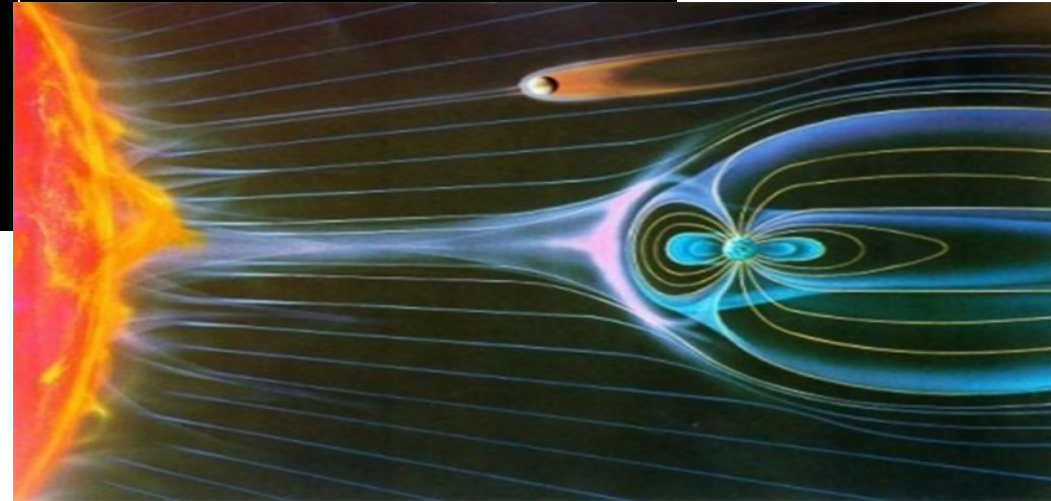
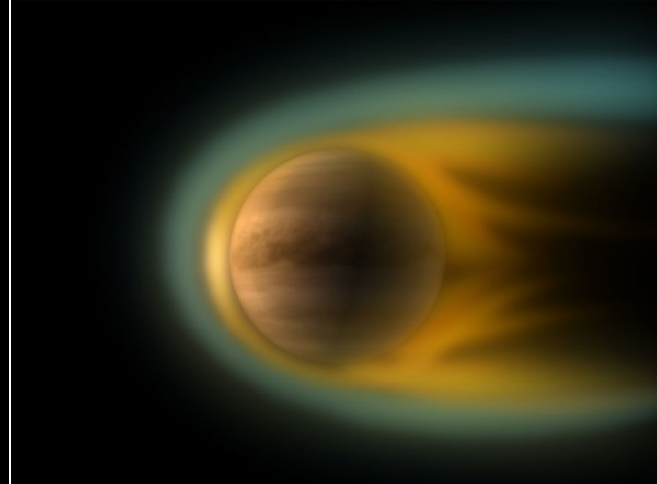


Auroras are found on most of the planets in the Solar system, magnetized or not.

Mercury (Mariner, Messenger probes)



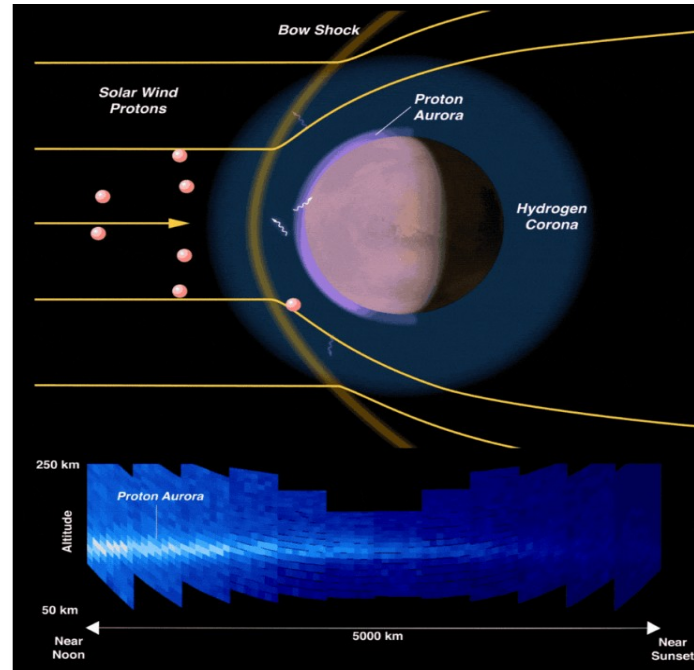
Venus



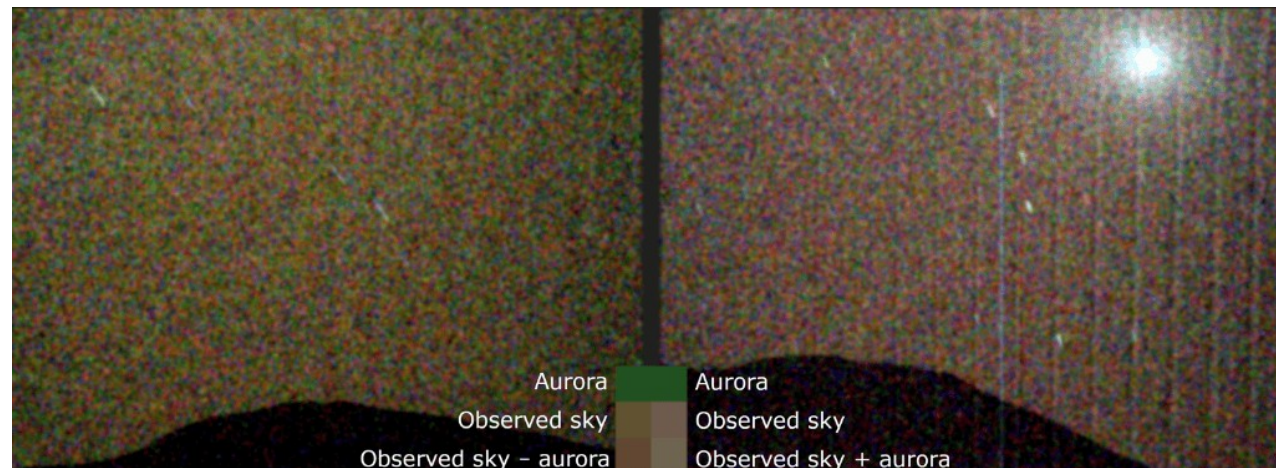
Venus has smaller aurora towards the Sun than is the case with Earth.



Even in the planets like Venus or Mars, which do not have significant magnetic field, we observe aurora, formed as a result of interaction of particles-here mostly protons- from the solar wind shock where the planet moves through the wind. It is most visible at the sunny side of the planet.

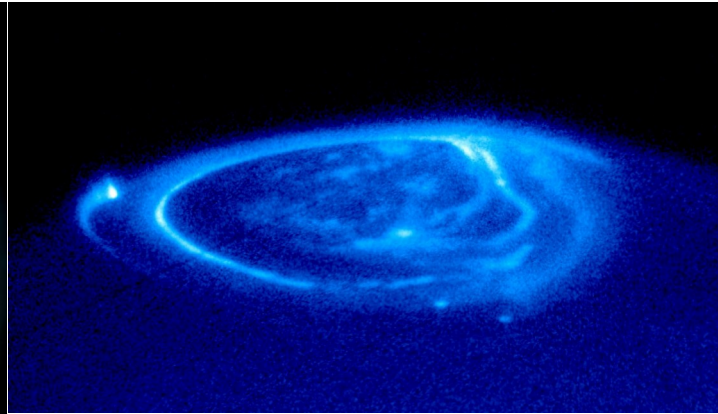
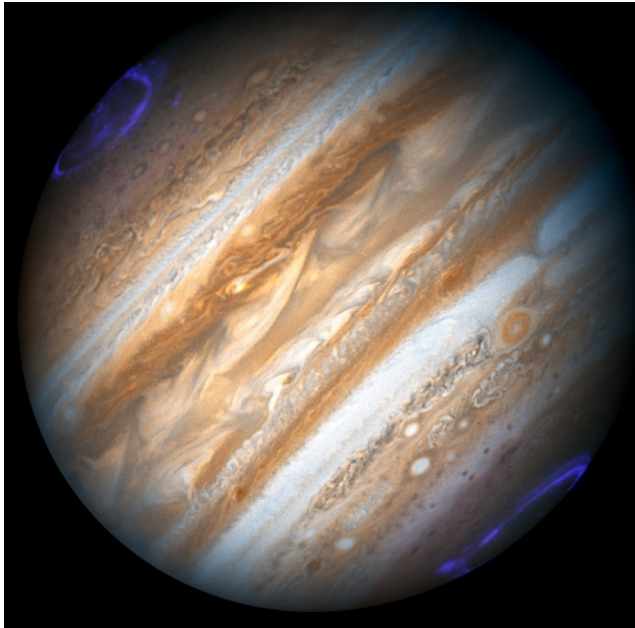


In March 2024, NASA Mars rover Perseverance made the first on-site observation of aurora from another planet-the greenish hue in the left panel:





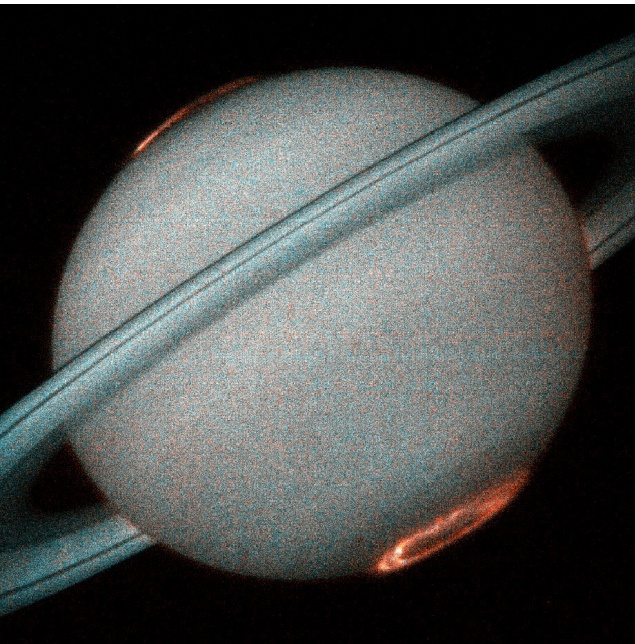
Aurora is observed also on Jupiter and Saturn. On the gas planets aurora is visible mostly in ultra-violet, so we can observe it from outside our atmosphere.



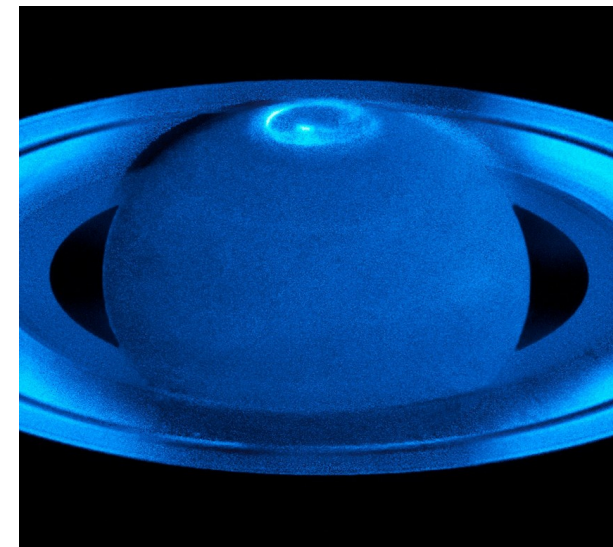
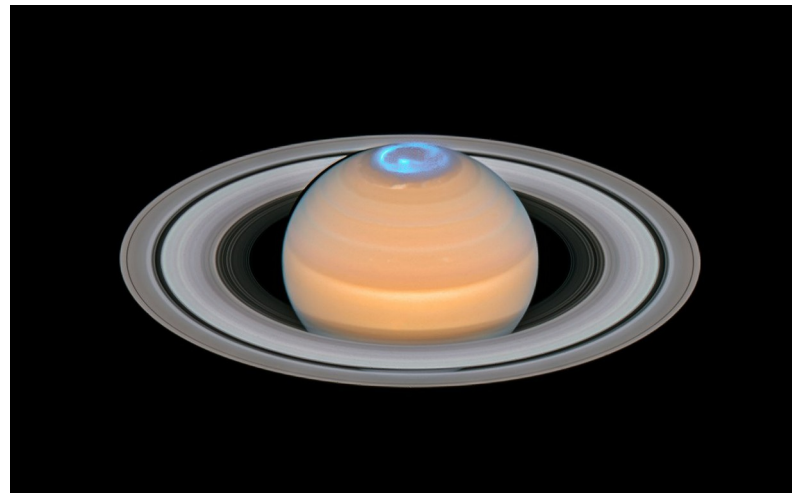
Spots in aurora on Jupiter are magnetically connected with its satellites: the spot on the left side is connected with Io, bottom two with Ganymede and Europe.



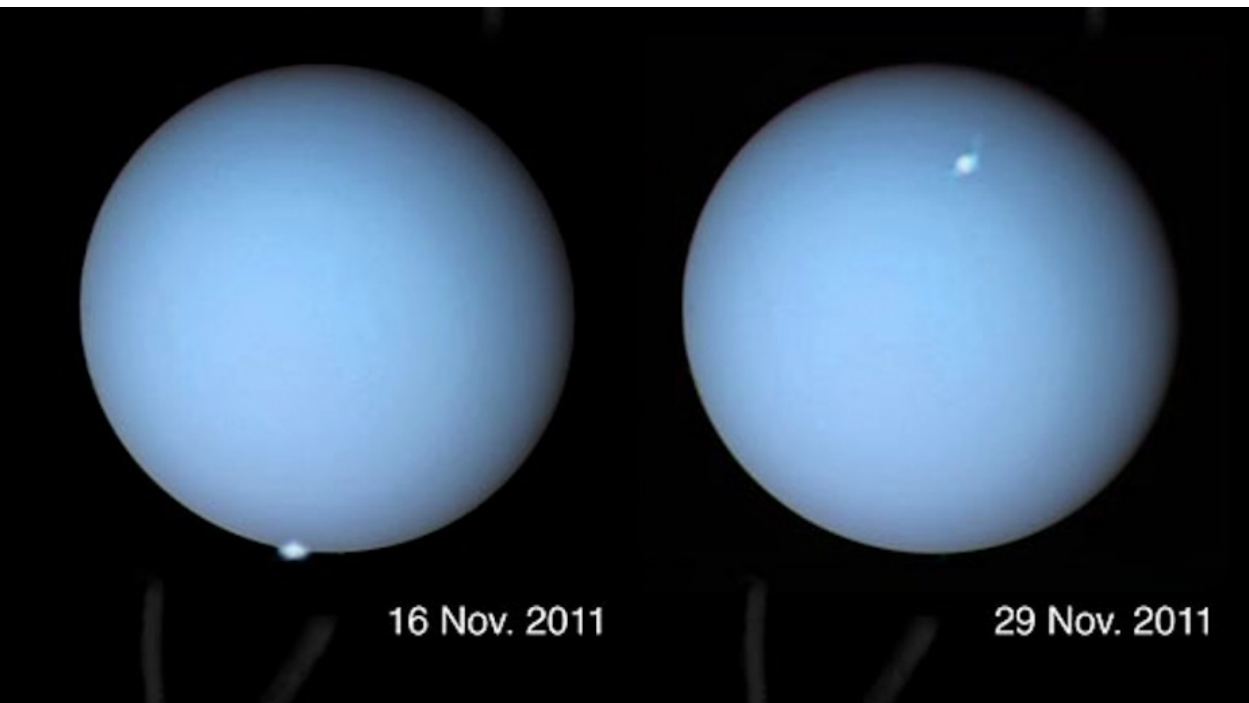
JWST's capture of aurora on Jupiter



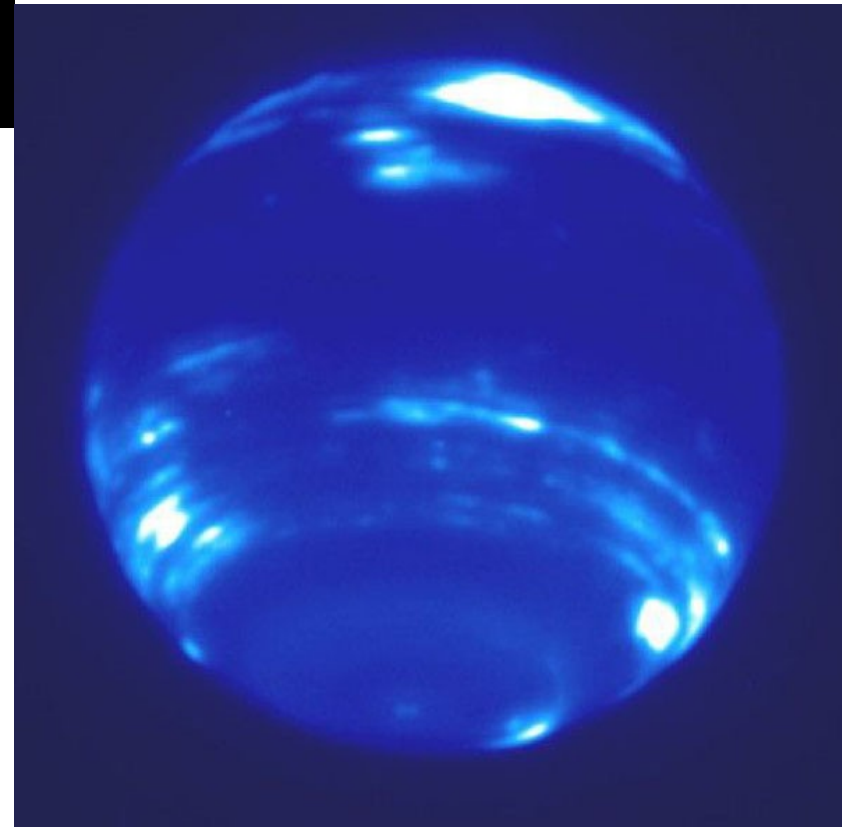
Saturn also features polar aurora:



HST observed auroras on Uranus:

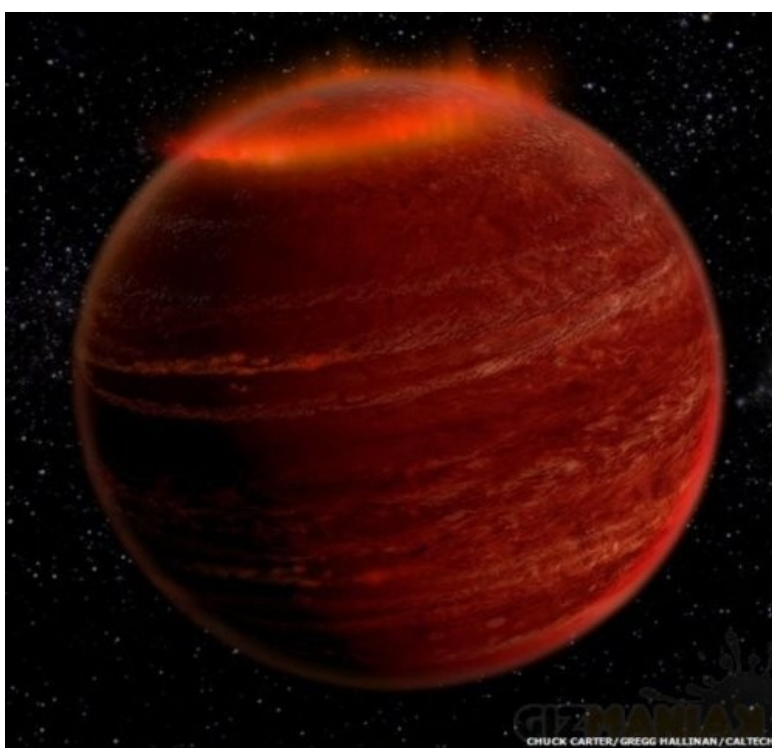


Keck observed it on Neptune:





- On exoplanets we also can expect auroras, but **there is yet no confirmed extrasolar aurora observation**. There are tentative observations, like on a brown M-dwarf LSR J1835+3259, 18 lyrs from us, in Lyra (artist impression shown below, of a reddish aurora, from more hydrogen in the atmosphere, and about million times more intense than on Earth, because of larger magnetic field). There are more of similar objects which show characteristic spectral features which point to aurora.
- Such an aurora should also be of different nature, because there is no other star for producing the stellar wind.
- A model for aurora requires a continuously adding plasma within the magnetosphere. This mass-loading can be achieved in multiple ways, including interaction with the interstellar medium, a volcanic activity on the orbiting planet embedded within the magnetosphere, or magnetic reconnection at the photosphere, or particles from the stellar wind producing the emanations from the planetary surface, like on Mercury.



In the cases of **planets around pulsars**, we can expect similar effects. Because of much larger pulsar magnetic field, and difference in pulsar wind ver. stellar wind, they could behave different from usual planet aurora.

**We made the first such model**, by introducing necessary modifications in the ordinary star - planet interaction setup.



- In a series of works by Varela et al. (e.g. A&A, 616, A182, 2018; A&A 659, A10, 2022) are given numerical simulations of planetary magnetospheric response in extreme solar wind conditions, using the PLUTO code.
- Such simulations are **tested for Mercury and Earth**, and are valid for exoplanets.

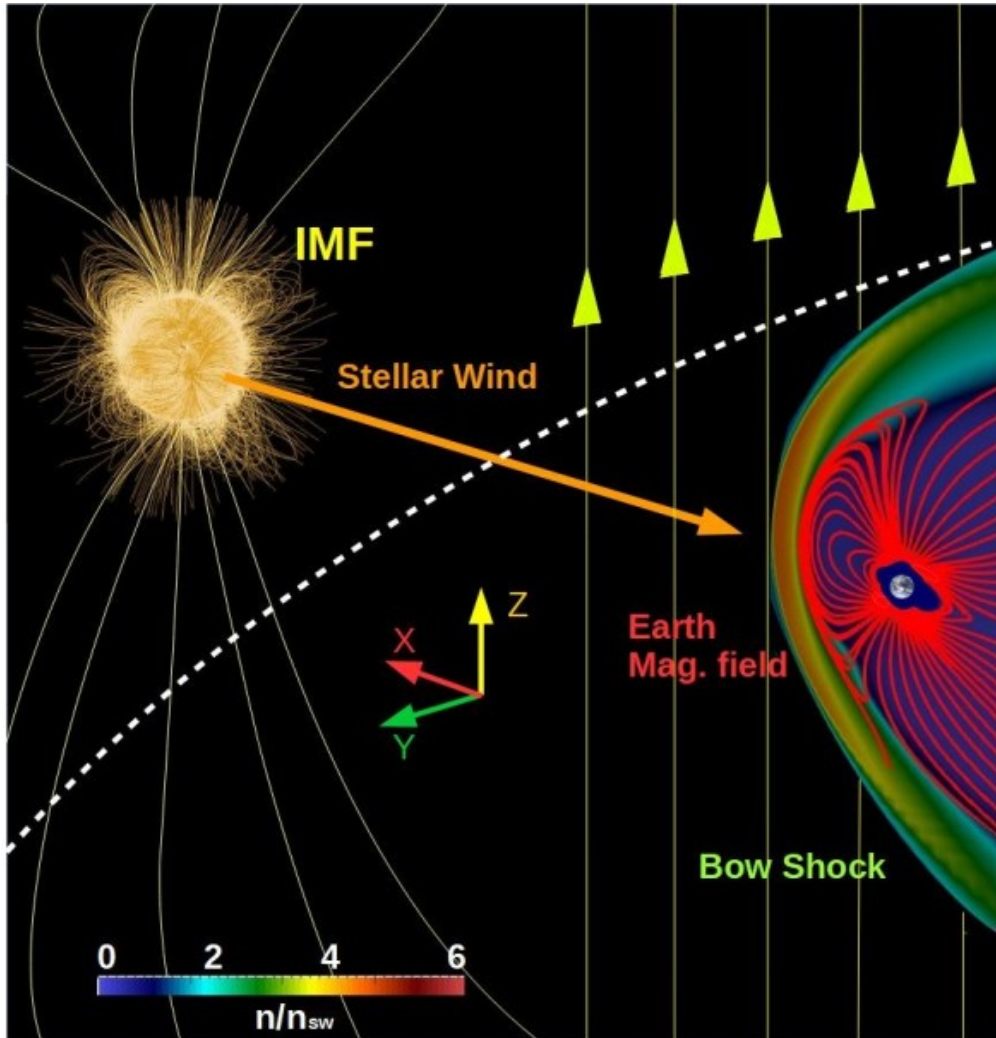


**Fig. 1.** 3D view of a typical simulation setup. We show the density distribution (color scale), Earth magnetic field lines (red lines), and IMF (yellow lines). The yellow arrows indicate the orientation of the IMF (northward orientation). The dashed white line shows the beginning of the simulation domain (the star is not included in the model).

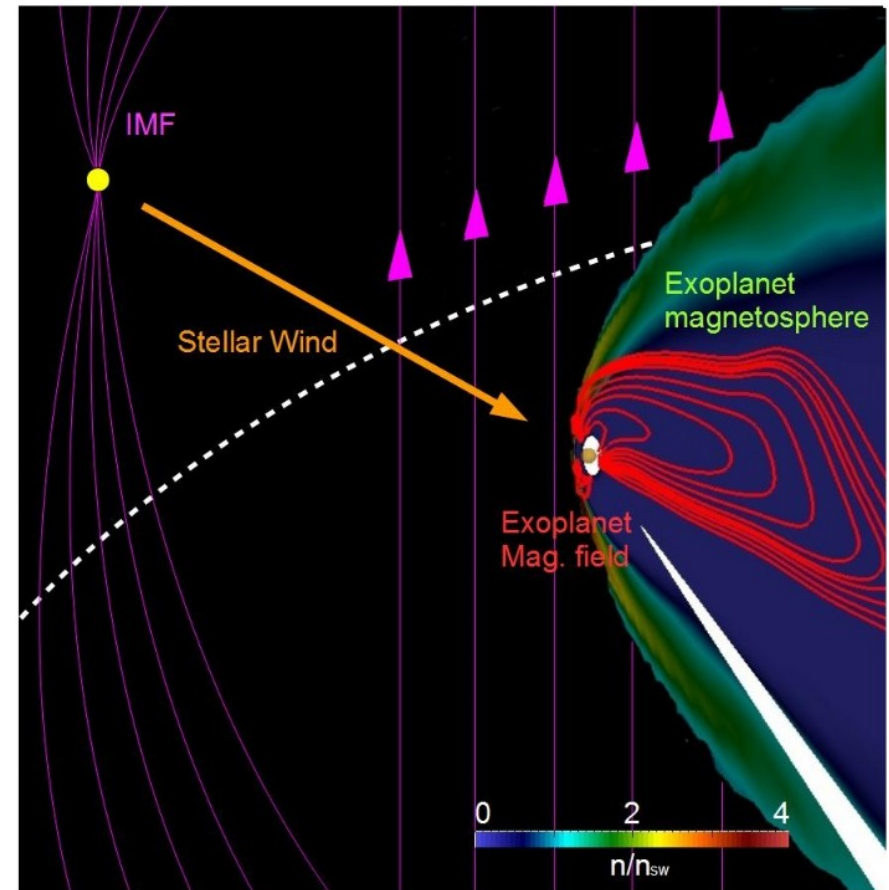


**Fig. 1.** 3D view of the system. Density distribution (color scale), field lines of the exoplanet magnetic field (red lines) and IMF (pink lines). The arrows indicate the orientation of the IMF (Northward orientation). Dashed white line shows the beginning of the simulation domain.

For Mercury we have a wealth of **data from Mariner 10** mission, which measured the dipole moment, and later **Messenger** mission, which provided more precise measurements for the multipolar representation.

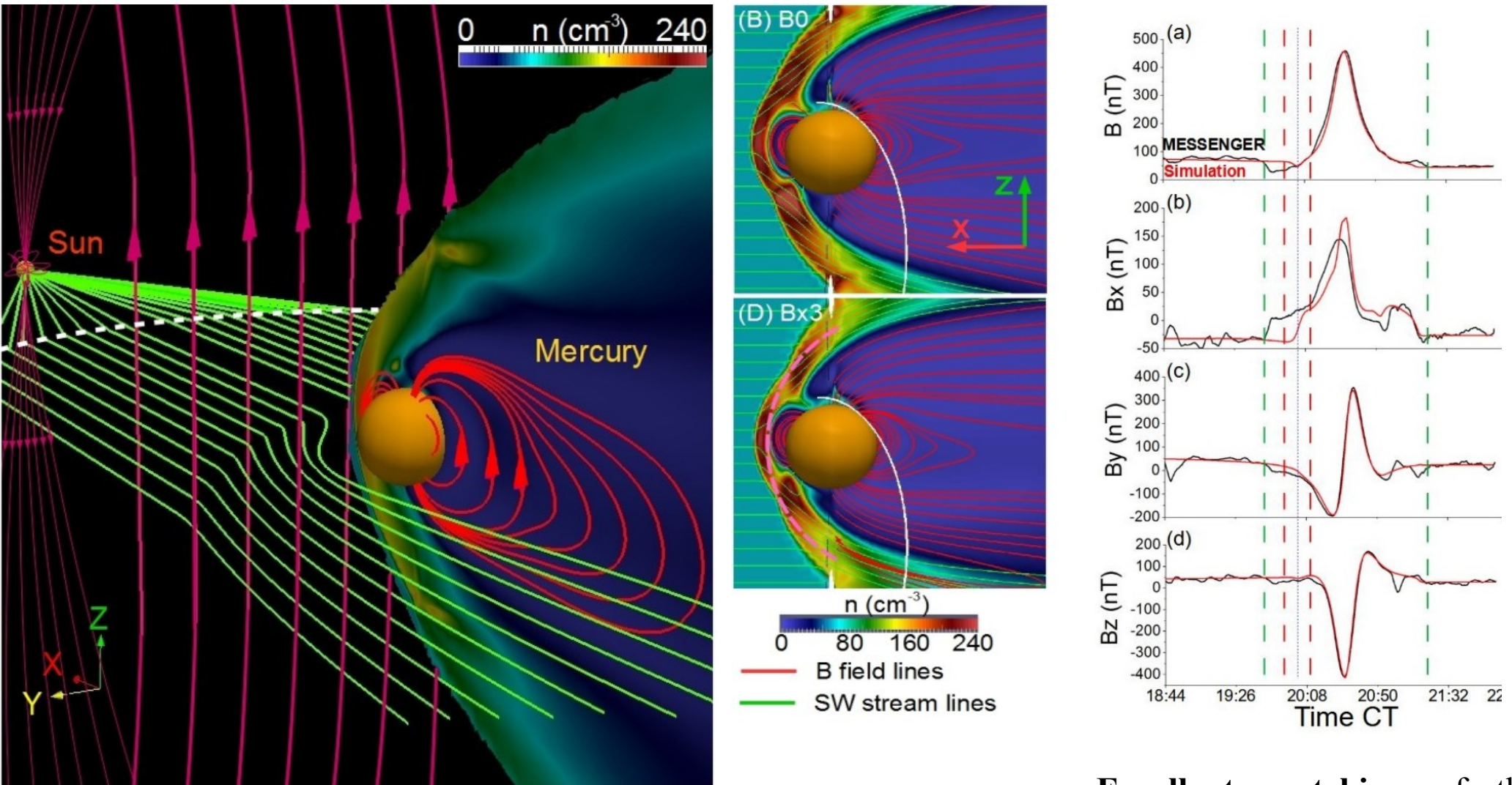
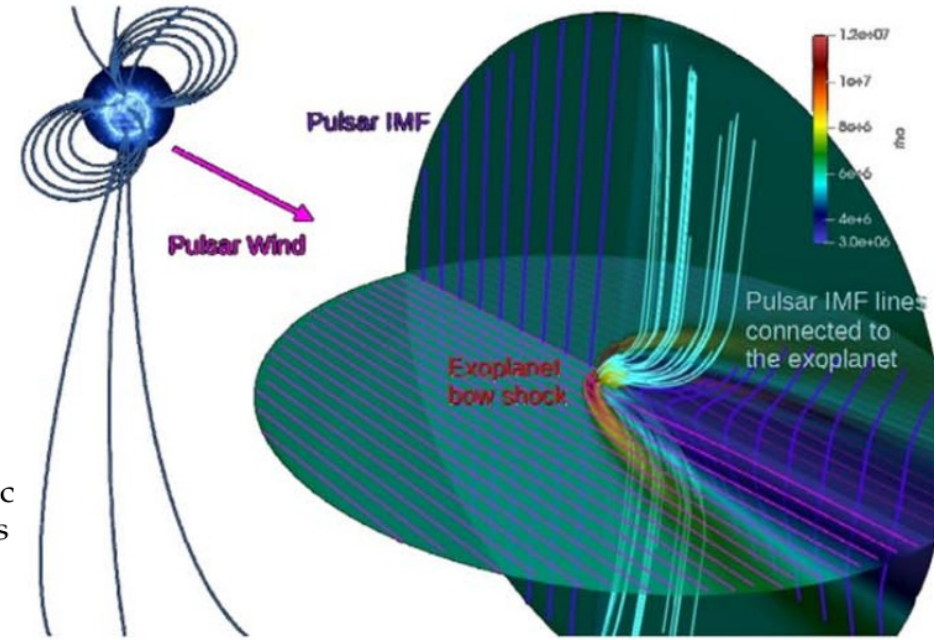


**Fig. 1.** 3D view of the system. Density distribution (color scale), field lines of the Hermean magnetic field (red lines), IMF (pink lines) and solar wind stream lines (green lines). The arrows indicate the orientation of the Hermean and interplanetary magnetic fields (case  $B_z$ ). Dashed white line shows the beginning of the simulation domain.

**Excellent matching** of the MESSENGER magnetometer data vs. simulation magnetic field along satellite trajectory.



This motivated our initial work in a direct non-relativistic analogy, but for more than initial study, we needed to include the fact that the pulsar wind is highly relativistic-so we used the relativistic module in the PLUTO code:



## 6.4 The RMHD Module

The RMHD module implements the equations of (ideal) special relativistic 1, 2 or 3 dimensions. Velocities are always assumed to be expressed in units and definition files are located inside the Src/RMHD directory.

The RMHD module solves the following system of conservation laws:

$$\frac{\partial}{\partial t} \begin{pmatrix} D \\ \mathbf{m} \\ E_t \\ \mathbf{B} \end{pmatrix} + \nabla \cdot \begin{pmatrix} D\mathbf{v} \\ w_t \gamma^2 \mathbf{v}\mathbf{v} - \mathbf{b}\mathbf{b} + p_t \\ \mathbf{m} \\ \mathbf{v}\mathbf{B} - \mathbf{B}\mathbf{v} \end{pmatrix}^T = \begin{pmatrix} 0 \\ \mathbf{f}_g \\ \mathbf{v} \cdot \mathbf{f}_g \\ 0 \end{pmatrix} \quad (6.13)$$

where  $D$  is the laboratory density,  $\mathbf{m}$  is the momentum density,  $E$  is the total energy (including contribution from the rest mass) while  $\mathbf{f}_g$  is an acceleration term (see [6.3](#)).

Primitive variables are similar to the RHD module but they also contain the magnetic field,  $\mathbf{V} = (\rho, \mathbf{v}, p, \mathbf{B})$ . The relation between  $\mathbf{V}$  and  $\mathbf{U}$  is

$$\begin{aligned} D &= \gamma \rho \\ \mathbf{m} &= w_t \gamma^2 \mathbf{v} - b^0 \mathbf{b} \\ E_t &= w_t \gamma^2 - b^0 b^0 - p_t \end{aligned} \quad , \quad \begin{cases} b^0 = \gamma \mathbf{v} \cdot \mathbf{B} \\ \mathbf{b} = \mathbf{B} / \gamma + \gamma (\mathbf{v} \cdot \mathbf{B}) \mathbf{v} \\ w_t = \rho h + \mathbf{B}^2 / \gamma^2 + (\mathbf{v} \cdot \mathbf{B})^2 \\ p_t = p + \frac{\mathbf{B}^2 / \gamma^2 + (\mathbf{v} \cdot \mathbf{B})^2}{2} \end{cases}$$

LOFAR was able to detect low-frequency radio waves that were predicted from a M-type dwarf GJ 1151 (or a planet around it) which is located 25 light-years from Earth (Vedantham et al. 2020). *This was, tentatively, the first signal detected from an extrasolar aurora.*

What are the numbers for Wolszczan's pulsar? The only case of star-planet interaction without non-thermal radio emission arises when both the planet and stellar wind are non-magnetized. In all the other cases, **even without intrinsic planetary magnetic field**, there can arise intense radio emission. Based on the observations of magnetized planets in the Solar system, the empirical estimate of the intensity of radio emission by Radiometric Bode's law (RBL), with the emission roughly proportional to the power from the stellar wind is:

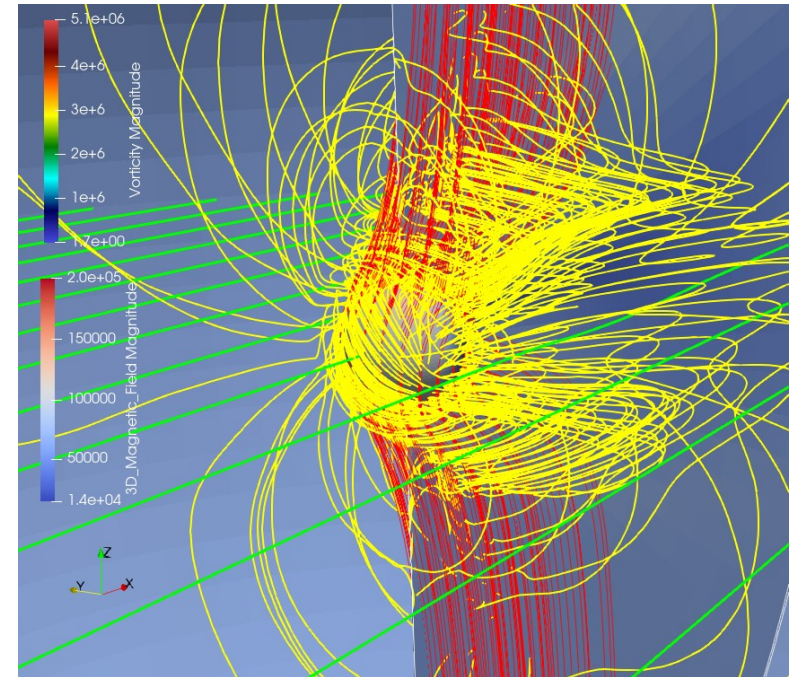
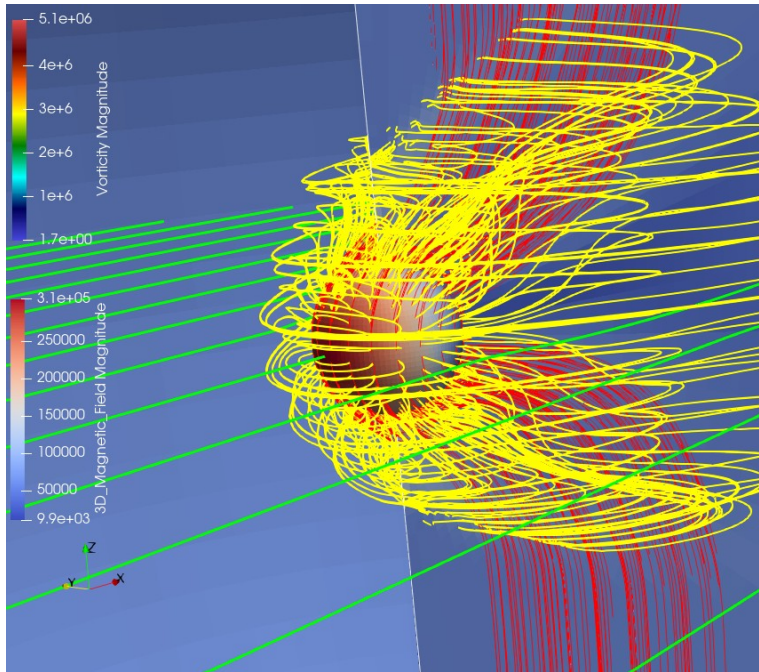
$$\nu_{\min} = \sqrt{\frac{ne^2}{\pi m_e}} \sim 8.98 \text{ kHz} \sqrt{n}, \quad \nu_{\max} = \frac{eB_{sw}}{2\pi m_e} \sim 2.8 \text{ MHz} B_{sw},$$

$$\Phi = \frac{P_{\text{rad}}}{\Omega d^2 \Delta\nu},$$

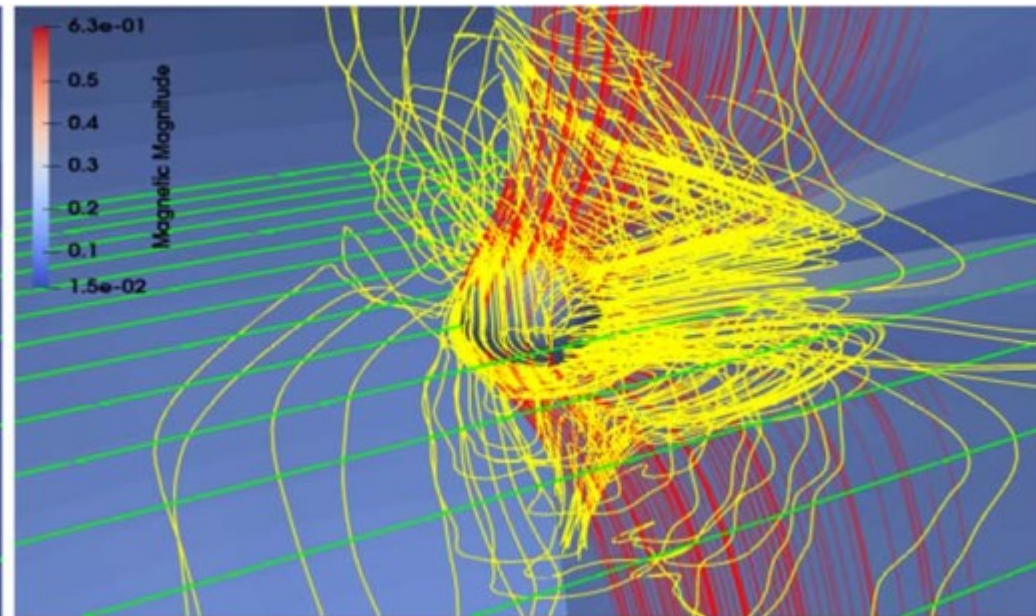
In the pulsar planet case, we considered rocky planets, as in Wolszczan's system, and assumed that they are not magnetized, or are negligibly magnetized, in comparison to the large magnetic field induced by the field carried in by the pulsar wind. Two simplest cases of the planetary surfaces are conductive and ferromagnetic. Simulation setups in the two cases are different only in conditions for magnetic field components at the planetary surface.



In the left and right panels are conductive and ferromagnetic cases, respectively. Non-relativistic cases:

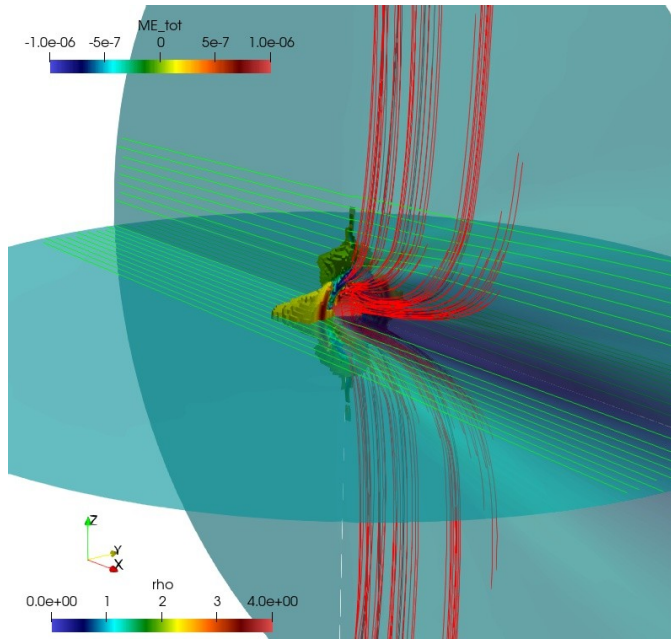


Relativistic cases are qualitatively similar:

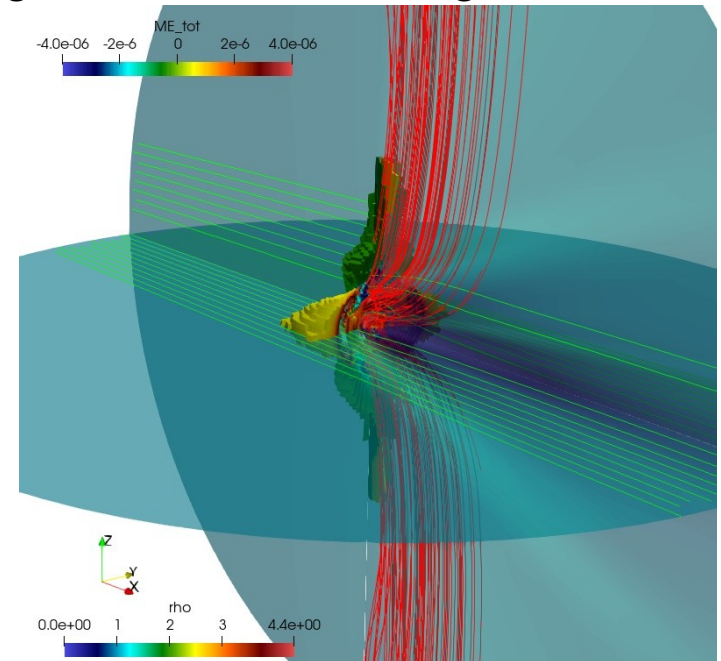




Conductive case

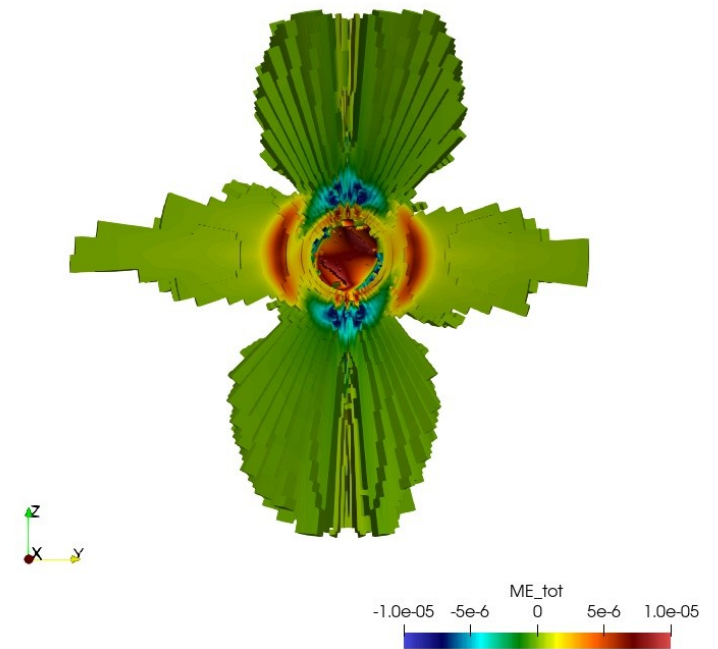
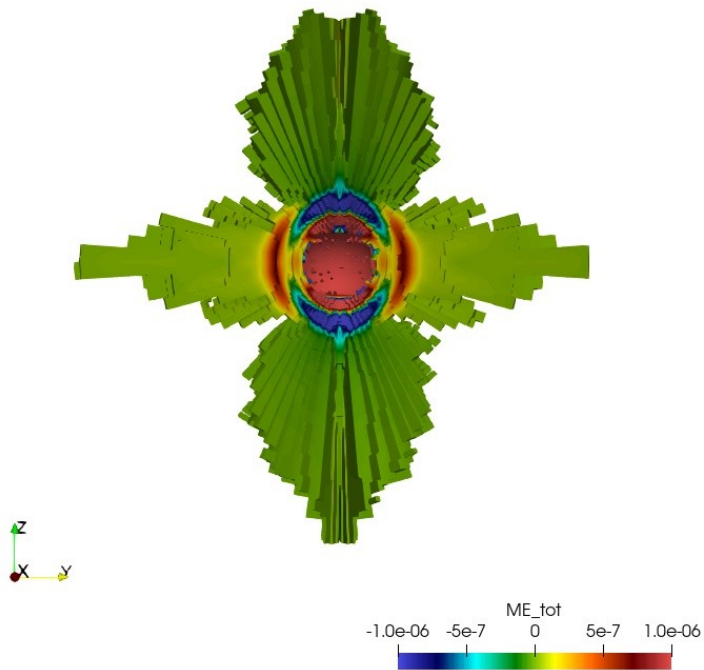


Iso volume of Poynting flux divergence



Ferromagnetic case

Magnetic power:



In the case with a main sequence star case, the flow carried protons, and in the pulsar wind, the flow is electron-positron plasma. The pulsar wind is much faster,  $0.87c$ .

**Table 1.** Parameters used in PLUTO setup file `pluto.ini` in our simulations for pulsar-planet setups with conductive and ferromagnetic planetary surfaces in comparison to Sun-Earth (CME) and Sun-Earth and Sun-Mercury (quiet) conditions. SW (Speed, MagField, Dens, and Temp) are setting the related initial values—in the Pulsar-planet case, SW corresponds to stellar or pulsar wind. PlanTemp sets the planetary temperature, and the Alfvén speed is limited by the `AlfSpeedLimit`. The radii  $R_{in}$  and  $R_{sw,cut}$  set the inner boundary of the system and the radial position of the nose of the bow shock at the beginning of the simulation, respectively. The density floor is controlled by `dens_min`= $0.01 \times \text{SWDens}$ .

Set-up	SWSpeed ( $\text{cm s}^{-1}$ )	SWMagField (G)	SWDens ( $\text{g cm}^{-3}$ )	SWTemp (K)	PlanTemp (K)	AlfSpeedLimit ( $\text{cm s}^{-1}$ )	$R_{in}$ ( $R_{NS}$ )	$R_{sw,cut}$ ( $R_{NS}$ )
Pulsar-planet (cond.)	$2.6 \times 10^{10}$	$2.5 \times 10^{-3}$	$5.0 \times 10^{-26}$	$5.0 \times 10^8$	-	-	1.0	-
Pulsar-planet (ferro)	$2.6 \times 10^{10}$	$1.0 \times 10^{-2}$	$1.0 \times 10^{-24}$	$5.0 \times 10^8$	-	-	1.0	-
Sun-Earth (CME)	$1.0 \times 10^8$	$1.0 \times 10^{-3}$	$3.0 \times 10^{-23}$	$1.0 \times 10^5$	$1.0 \times 10^3$	$5.0 \times 10^8$	3.0	6.0
Sun-Earth (quiet)	$3.5 \times 10^7$	$5.0 \times 10^{-5}$	$6.0 \times 10^{-24}$	$4.0 \times 10^4$	$1.0 \times 10^3$	$5.0 \times 10^8$	3.0	6.0
Sun-Mercury (quiet)	$5.0 \times 10^7$	$1.5 \times 10^{-4}$	$2.0 \times 10^{-23}$	$8.0 \times 10^4$	$2.0 \times 10^3$	$1.0 \times 10^8$	1.0	3.0

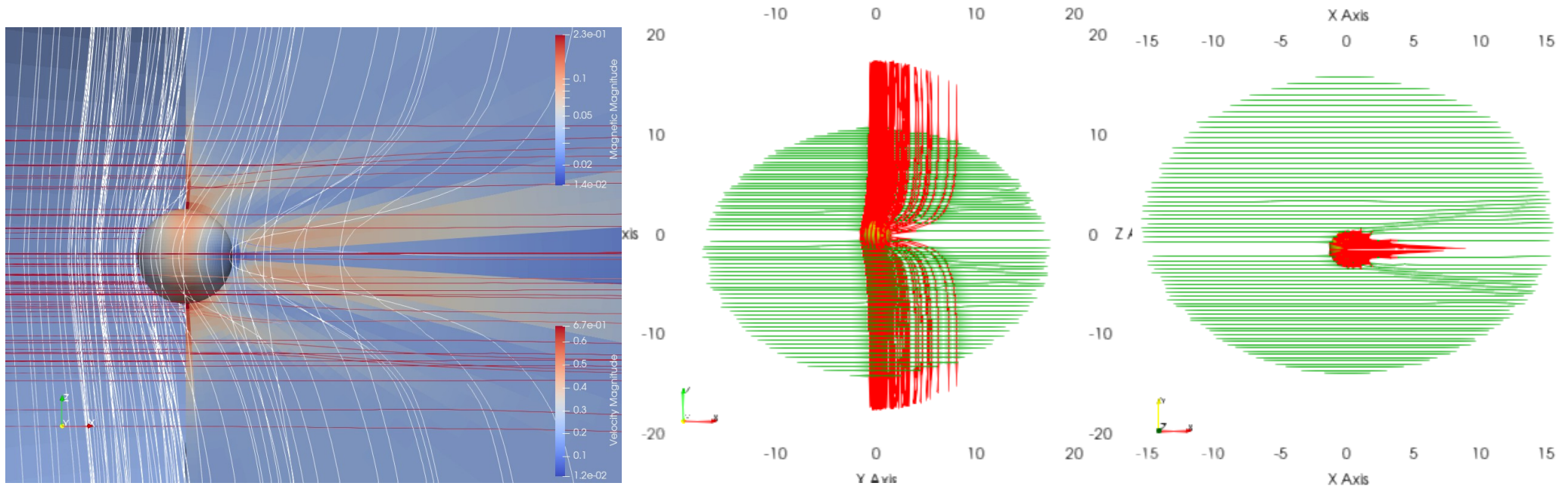


Table 2. Predicted and tentative intensity of the radio emission flux  $\Phi$  for an observer on Earth in our two simulations with non-magnetized pulsar planet with conducting and ferromagnetic planetary surfaces, at different distances (in parsecs) from us. In the last three columns we check if the predicted values are above the frequency limit *AND* sensitivity of the currently most sensitive instruments, LOFAR and MeerKAT, and the future SKA. We also estimate the tentative realistic results in each of the cases, which indicate that such objects could be observable today.

Set-up	$\Phi_a(750)$ (mJy)	$\Phi_b(250)$ (mJy)	$\Phi_c(100)$ (mJy)	$P_{radio}$ (Wm <sup>-2</sup> )	$B_{sw}$ (G)	$\Delta\nu$ MHz	LOFAR	MeerKAT	SKA
Pulsar-planet (cond.)	0.60	5.4	33.75	$3.65 \times 10^{12}$	0.0025	0.007	NO	NO	NO
Tentative	>	>	>	>	7.4	20.1	YES	YES	YES
Pulsar-planet (ferrom.)	0.47	4.23	26.43	$1.14 \times 10^{13}$	0.01	0.028	NO	NO	NO
Tentative	>	>	>	>	13	36.4	YES	YES	YES



In the EAS 2023 meeting in Cracow in July 2023, where PhD student Ruchi Mishra, who worked with us on the article, had a poster with our results, I met Alex Wolszczan, the discoverer of the first exoplanets, around a pulsar and asked him what he thinks of our idea about auroras on his planets. He listened carefully and commented: “I did not come to such an idea. Give numbers!” Exactly this is what we did in the paper, making a challenge to the observers:

THE ASTROPHYSICAL JOURNAL LETTERS, 959:L13 (6pp), 2023 December 10

© 2023. The Author(s). Published by the American Astronomical Society.

OPEN ACCESS

<https://doi.org/10.3847/2041-8213/ad0f1f>



## Auroras on Planets around Pulsars

Ruchi Mishra<sup>1</sup> , Miljenko Čemeljić<sup>1,2,3</sup> , Jacobo Varela<sup>4</sup> , and Maurizio Falanga<sup>5,6</sup>

<sup>1</sup> Nicolaus Copernicus Astronomical Center of the Polish Academy of Sciences, Bartycka 18, 00-716 Warsaw, Poland

<sup>2</sup> Research Centre for Computational Physics and Data Processing, Institute of Physics, Silesian University in Opava, Bezručovo nám. 13, CZ-746 01 Opava, Czech Republic

<sup>3</sup> Academia Sinica, Institute of Astronomy and Astrophysics, P.O. Box 23-141, Taipei 106, Taiwan

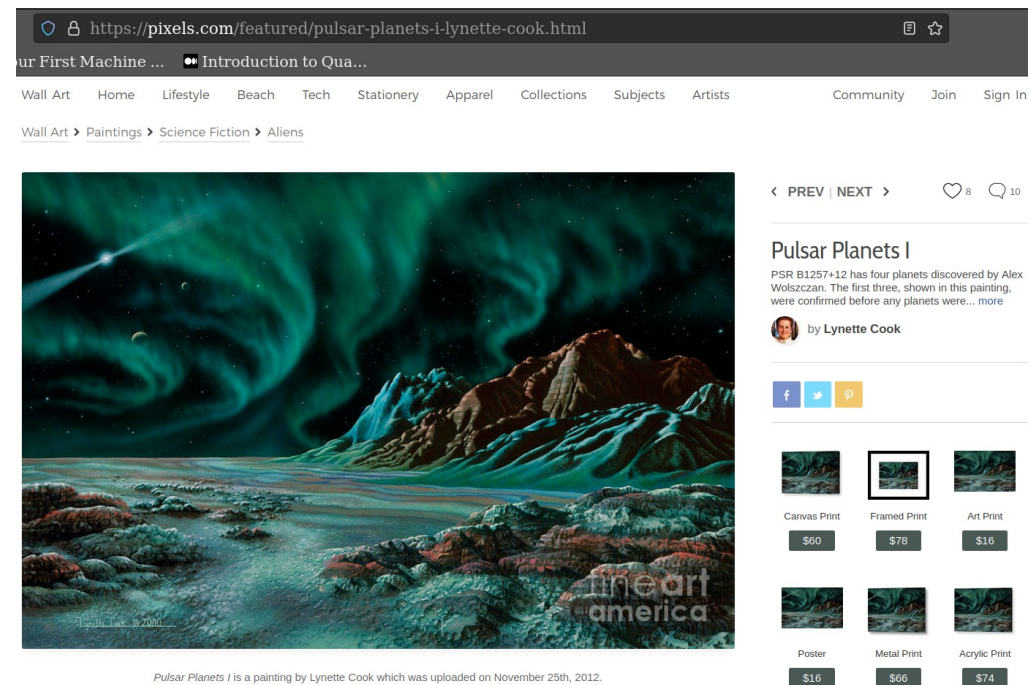
<sup>4</sup> Universidad Carlos III de Madrid, Leganes, E-28911, Spain

<sup>5</sup> International Space Science Institute, Hallerstrasse 6, 3012 Bern, Switzerland

<sup>6</sup> Physikalisches Institut, University of Bern, Sidlerstrasse 5, 3012 Bern, Switzerland

Received 2023 September 12; revised 2023 November 14; accepted 2023 November 22; published 2023 December 14

But there was an interesting twist to the story. During the New Year break, browsing for “pulsar planets aurora” for a content related to our paper freshly published in December, I was stunned to find the following picture, titled “Pulsar planets 1”:



Pulsar Planets I is a painting by Lynette Cook which was uploaded on November 25th, 2012.

The posting date, 2012 and, on closer inspection, an even earlier date on the picture, **2000** was intriguing.

I contacted the artist, Ms. Lynette Cook, an accomplished scientific illustrator, asking if she just made it by analogy with Earth aurora? She answered that no, she asked Alex Wolszczan back in 1999 about the scientific plausibility of the painting for illustration of an article about his planets, and he suggested her to add an aurora! She showed the picture in many exhibitions.

So, it seems Alex Wolszczan did have an artistic idea of it, which did not pass into the scientific work. Our work is the first where it is computed...almost a quarter of century after the painting!





This prompted me to search again for mentioning of such auroras, and the only result I found was a few words in a conference proceedings, without any follow-up:

EPSC Abstracts  
Vol. 11, EPSC2017-623-1, 2017  
European Planetary Science Congress 2017  
© Author(s) 2017



## Feasibility and benefits of pulsar planet characterization

**J. Nekola Novakova** (1,2) and T. Petrasek (1,3)

(1) Charles University, Czech Republic: Faculty of Mathematics and Physics, Department of Geophysics, (2) Charles University, Czech Republic: Faculty of Science, (3) Academy of Sciences, Czech Republic; ([julie.novakova@natur.cuni.cz](mailto:julie.novakova@natur.cuni.cz))

### Abstract

Planet orbiting neutron stars seem to be rare, but all the more interesting for science due to their origins. Characterizing the composition of pulsar planets could elucidate processes involved in supernova fallback disks, accretion of companion star material, potential survival of planetary cores in the post-MS phase of their stars, and more. However, the small size and unusual spectral distribution of neutron stars (NS) make any spectroscopic measurements very difficult if not impossible in the near future. In this work, we set to estimate the feasibility of spectroscopy of planets orbiting specifically pulsars, and to review other possible methods of characterization of the planets, such as emissions caused by aurorae.

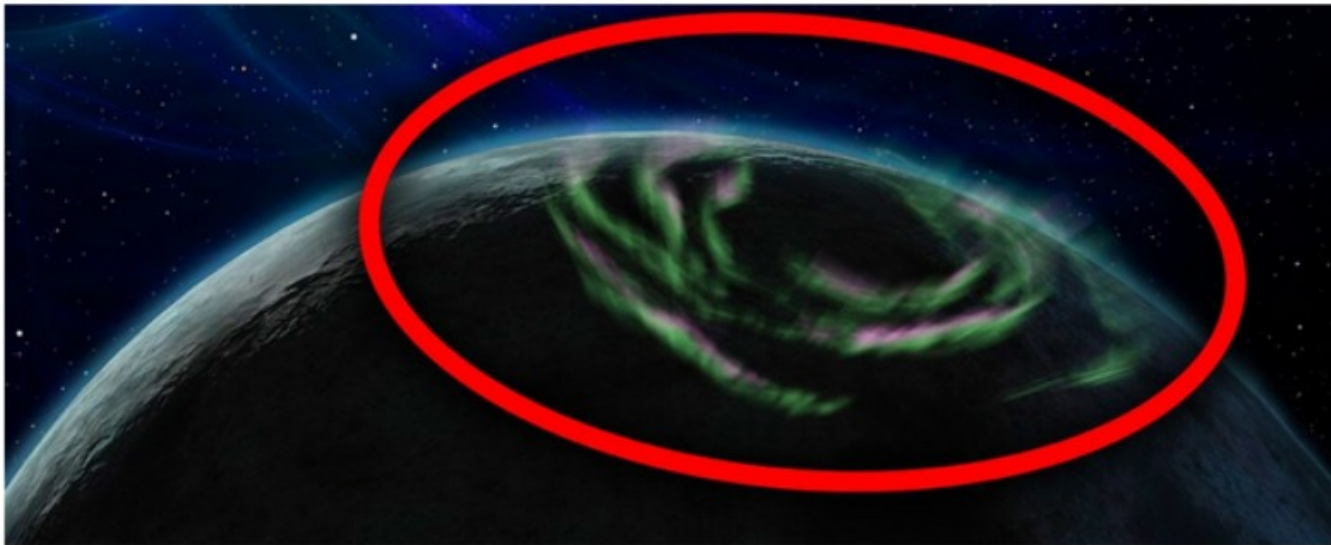
circumstellar disk of the magnetar 4U 0142+61 [9], and a tentative asteroid belt around the millisecond pulsar B1937+21 [7]. PSR B1620-26 b is a circumbinary planet orbiting a pulsar and a white dwarf, and likely formed around the white dwarf precursor, with its system later captured by the pulsar, giving rise to a binary, while the pulsar's original stellar companion was ejected [8]. In a globular cluster with high star density, where this system is present, such an event is more likely than in the galactic disk. Finally, the PSR J1719-1438 system contains most likely a remnant of a disrupted WD companion that narrowly avoided its complete destruction, based on its minimum density [1].

These three known systems represent three of the possible means of origin of pulsar planets. Formation in disks from WD-NS mergers as opposed to

In a new [paper](#) published on 7 December by a team of Swiss scientists, they propose that exoplanets around pulsars may well experience aurora by simulating their magnetic environment.

# Strange And Beautiful Auroras May Glow on Planets Orbiting Pulsars

SPACE 17 December 2023 By MARK THOMPSON, UNIVERSE TODAY



Artist's impression of auroras on a planet orbiting a pulsar. (Universe Today)

We have been treated to some amazing aurora displays over recent months. The enigmatic lights are caused by charged particles from the Sun rushing across space and on arrival, causing the gas in the atmosphere to glow.

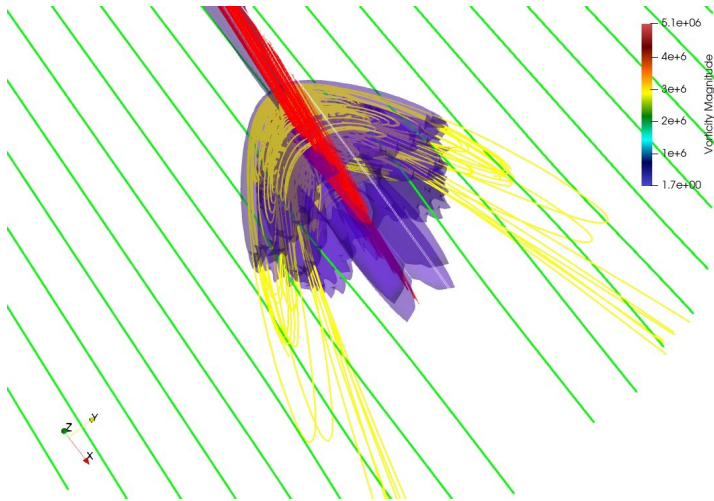
Now researchers believe that even on exoplanets around [pulsars](#) we may just find aurora, and they may even be detectable.



In the first paper we could not reach the pulsar wind speed larger than  $0.87c$ , while  $>0.99c$  is needed.

With the theoretical collaboration and discussions with **Sergio Joya** finishing his Master studies here in Bern, our PhD student in Warsaw, **Tanja Kaister**, managed to extend our simulations to the super-relativistic regime, with pulsar wind reaching  $0.985c$ . This is a preparatory work for further publication where we plan to give more information needed for observations, in collaboration with **Piyush Marmat**, a PhD student in Torun, Poland, who also collaborated with Maurizio Falanga.

The results confirm our assumptions from the first paper, about the increased emission with the further increased pulsar wind speed.



Equatorial view-Alfven “wings” in non-relativistic flow in our simulations. How this changes in super-relativistic flow?

-Mottez & Heyvaerts (2011a,b) worked on planets around pulsars in the context of theory of electromagnetic interaction of stars and planets or small bodies. They extended the theory of Alfvén wings to relativistic winds. I leave this to Sergio Joya, who, working with Maurizio Falanga in Bern on his MS Thesis, contributed to our work by investigating the planets as obstacle in relativistic flow.

## Planets in Pulsar Winds

T. Kaister<sup>1</sup>, S. Andrés Joya Méndez<sup>2</sup>, P. Marmat<sup>3</sup>, M. Čemeljić<sup>3,1,4</sup>, M. Velli<sup>6</sup>, and J. Varela<sup>7</sup>

<sup>1</sup> Nicolaus Copernicus Astronomical Center, Polish Academy of Sciences, Bartycka 18, 00-716, Warsaw, Poland  
e-mail: tkaister@camk.edu.pl

<sup>2</sup> Physikalisches Institut, University of Bern, Sidlerstrasse 5, 3012 Bern, Switzerland

<sup>3</sup> Nicolaus Copernicus Superior School, College of Astronomy and Natural Sciences, Gregorkiewicza 3, 87-100, Toruń, Poland

<sup>4</sup> Research Centre for Computational Physics and Data Processing, Institute of Physics, Silesian University in Opava, Bezručovo nám. 13, CZ-746 01 Opava, Czech Republic

<sup>5</sup> Department of Earth, Planetary, and Space Sciences, University of California–Los Angeles, Los Angeles, CA 90056, USA

<sup>6</sup> Institute for Fusion Studies, Department of Physics, University of Texas at Austin, Austin, Texas 78712, USA

### ABSTRACT

This work presents the results of a simulation of a planet in a pulsar wind of velocity  $v = 0.985c$ , which corresponds to a Lorentz factor  $\gamma = 5.795$ . The planet was modeled as a perfect conductor in an external magnetic field originating from the pulsar. The results show that the pulsar wind bends the magnetic field lines around the planet and that an electric dipole forms. It is also shown that radio emission is expected to be produced in the magnetotail.

# Theoretical Aspects Pulsar - Planet Interactions

Following previous works from Mottez, Heyvaerts, and Zarka. The steps to follow in order to understand the Pulsar - Planet Interaction and the creation of aurora are the following:

- (1) Understanding all possible types of interaction of a plasma flow with an obstacle
- (2) Studying the more similar known interaction that better suits the model (Jupiter - Io)
- (3) Extrapolate relativistically the best known interaction for our case (Pulsar - Planet)
- (4) Predict flux densities or emitted radio power via comparison (Bode's Law)
- (5) Compare predicted flux densities with simulated outcomes using PLUTO



# (1) Possible Types of Flow - Obstacle Interactions

<sup>a</sup>Flow magnetic field  $|\mathbf{B}|$ :  $\uparrow$  = strong,  $\downarrow$  = weak (the solar wind is weakly magnetized).

<sup>b</sup> $M_A$ :  $\uparrow$  = super-Alfvénic,  $\downarrow$  = sub-Alfvénic

<sup>c</sup>Cyclotron maser instability

<sup>d</sup>AW Alfvén wings, UI unipolar inductor

**Table 1** Possible types of flow-obstacle interactions, examples, radio signatures, and extrapolation to star-planet plasma interactions

Flow $ \mathbf{B} ^a$	Flow $M_A^b$	Obstacle	Known examples in the solar system (mechanism) <i>Expected star-planet interaction (mechanism)</i>	Observed CMI <sup>c</sup> radio signature <i>Expected CMI radio signature</i>
$ \mathbf{B}  \downarrow$	$\uparrow$	<b>B</b>	Solar wind – planet: Mercury, Earth, Jupiter, Saturn, Uranus, Neptune → magnetospheres (reconnection) <i>Stellar wind – magnetized exoplanet (reconnection)</i>	From planet's aurora (Earth, Jupiter, Saturn, Uranus, Neptune) <i>From exoplanet's aurora</i>
$ \mathbf{B}  \downarrow$	$\downarrow$	<b>B</b>	– <i>Stellar wind – magnetized hot jupiter (reconnection)</i>	– <i>From exoplanet's aurora</i>
$ \mathbf{B}  \downarrow$	$\uparrow$	No <b>B</b>	Solar wind – insulating obstacle: Moon, Asteroids [rocky] (flow absorption, no shock, wake) <i>Stellar wind – unmagnetized exoplanet (induced magnetosphere)</i>	– – –
$ \mathbf{B}  \downarrow$	$\downarrow$	No <b>B</b>	Saturn – satellites (AW/UI) <sup>d</sup> <i>Stellar wind – unmagnetized hot jupiter (AW/UI)</i>	– –

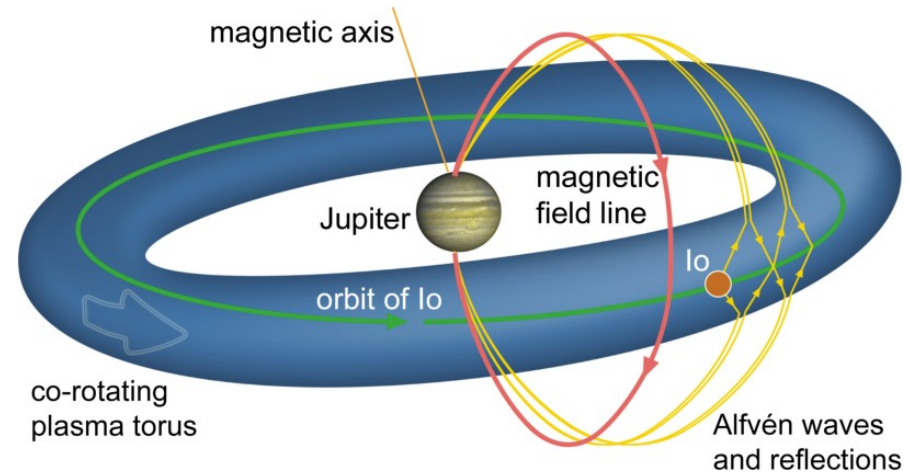
$ \mathbf{B}  \uparrow$	$\uparrow$	<b>B</b>	– <i>Magnetized star – magnetized exoplanet (reconnection)</i>	– <i>From exoplanet's aurora</i>
$ \mathbf{B}  \uparrow$	$\downarrow$	<b>B</b>	Jupiter – Ganymede (reconnection) <i>Magnetized star – magnetized hot jupiter (reconnection)</i>  <i>Pulsar – planet (reconnection)</i>	At Ganymede flux tube footprints <i>From exoplanet's aurora and/or at star-planet flux tube footprints</i> <i>In Alfvén wing → fast radio bursts?</i>
$ \mathbf{B}  \uparrow$	$\uparrow$	No <b>B</b>	– <i>Magnetized star – unmagnetized exoplanet (AW/UI → induced magnetosphere)</i>	– <i>Along magnetopause?</i>
$ \mathbf{B}  \uparrow$	$\downarrow$	No <b>B</b>	Jupiter – Io, Europa (AW/UI) <i>Magnetized star – unmagnetized hot jupiter (AW/UI)</i> <i>Pulsar – planet (AW/UI)</i>	At Io and Europa – flux tube footprints <i>At star-planet flux tube footprints</i> <i>In Alfvén wing → fast radio bursts?</i>
No <b>B</b>		<b>B</b>	Particle precipitations into cusp (low energy)	–
No <b>B</b>		No <b>B</b>	Plasma wake	–

## (2) Best Known Interaction for our Model (Jupiter - Io)

The model of our Pulsar-planet system is analogue to the Jupiter-Io system.

The satellite is weakly magnetized and its ionosphere interacts with the Jovian field through Alfvén waves and generates “wings”

The flow is sub-Alfvénic and the wings are the result from a “Unipolar Inductor” interaction studied by Drell et al. 1965 and Neubauer 1980.



Blöcker, Aljona. “Modeling Io's and Europa's Plasma Interaction with the Jovian Magnetosphere: Influence of Global Atmospheric Asymmetries and Plumes.” (2017).

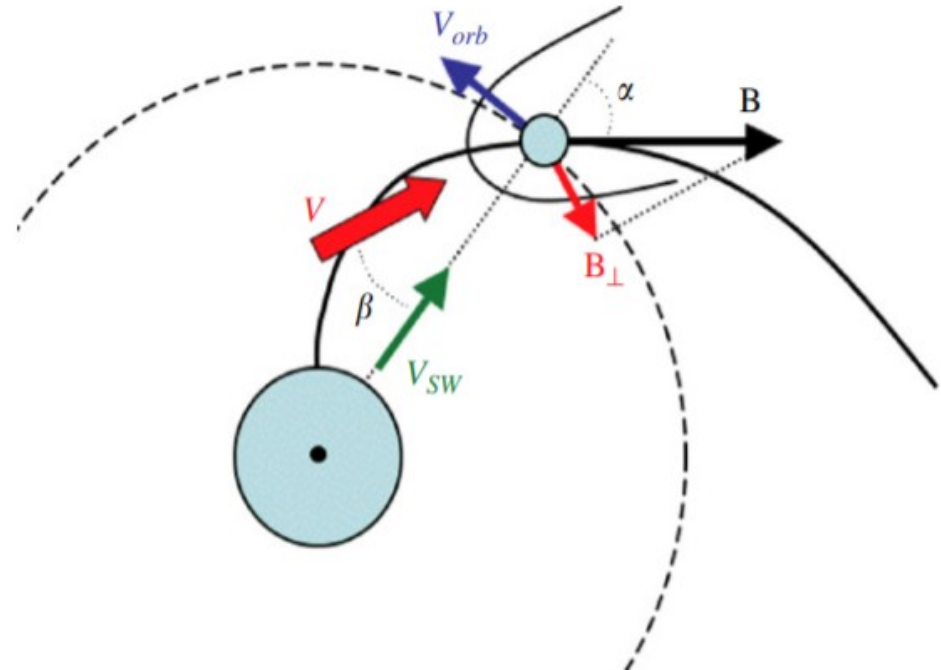


### (3) Extrapolate The Previous Interaction for the Relativistic Case

The equations of special-relativistic ideal MHD are used in order to extend the theory of Alfvén wings to relativistic winds.

The conclusions of the Jupiter - Io system are adapted to the relativistic inductor.

Neubauer (1989) found the total current / flowing along an Alfvén wing and the dissipation power involved in an Alfvén wing. Mottez & Heyvaerts 2011b do it for the relativistic case.



Sketch of the geometry of the Star wind flow and magnetic field at a planetary orbit (Zarka 2007)

# Proving that the Pulsar Wind is Sub-Alfvénic

The wind frame  $R_W$  corresponds to the instantaneous rest frame of the non-perturbed wind close to the planet. The quantities in  $R_W$  have a superscript  $x'$

In  $R_W$  the propagation velocity  $C'_A$  of Alfvénic perturbations takes the form:

$$C'_A = \frac{V'_A}{\sqrt{1 + \frac{V'^2_A}{c^2}}}$$

$$C'^{-2}_A = c^{-2} + V'^{-2}_A = c^{-2} + \frac{\mu_0 \rho'_0}{B_0'^2}$$

If the flow is sub-Alfvénic there is no bow shock and the obstacle is in direct contact with the pulsar wind. Otherwise, there is a shock wave that will modify the flow. In the model for aligned pulsars (Kirk et al. 2009), the wind is characterized by two invariants along its flow: the mass flux  $f$  and the pulsar magnetic flux  $\Psi$ . For cold radial flows and radial poloidal fields they are:

$$f = \gamma_0 \rho'_0 v_0^r r^2$$

$$\Psi = r^2 B_0^r$$

They come from the fact that the stationary equations of an axisymmetric perfect MHD flow allows a set of integrals of motion along stream lines.

$\sigma_0$  is the magnetization parameter defined by:

$$\sigma_0 = \frac{\Omega_*^2 \Psi^2}{\mu_0 f c^3} \quad (127)$$

and characterizes the ability of the field to launch the particles to high proper velocities. Since the pulsar wind is dominated by the highly relativistic Poynting flux:

$$\sigma_0 \gg 1 \quad (128)$$

The models show that (Mottez, F. and Heyvaerts, J. 2011):

$$\gamma_0 \longrightarrow \sigma^{1/3} \quad (129)$$

$$v_0^2 \longrightarrow \left(1 - \frac{1}{\sigma_0^{2/3}}\right) c^2 \quad (130)$$

$$V'_A \longrightarrow \left(1 - \frac{1}{2\sigma_0^{4/3}}\right) \quad (131)$$

Hence, by expanding around  $(1/\sigma_0)$ , to lower order, the value of  $M'_A$  is:

$$M'_A \longrightarrow \left(1 - \frac{1}{2\sigma_0^{4/3}}\right) \quad (132)$$

and so,  $v_0 < V'_A$ , which is the result wanted for the pulsar wind to be sub-Alfvénic.

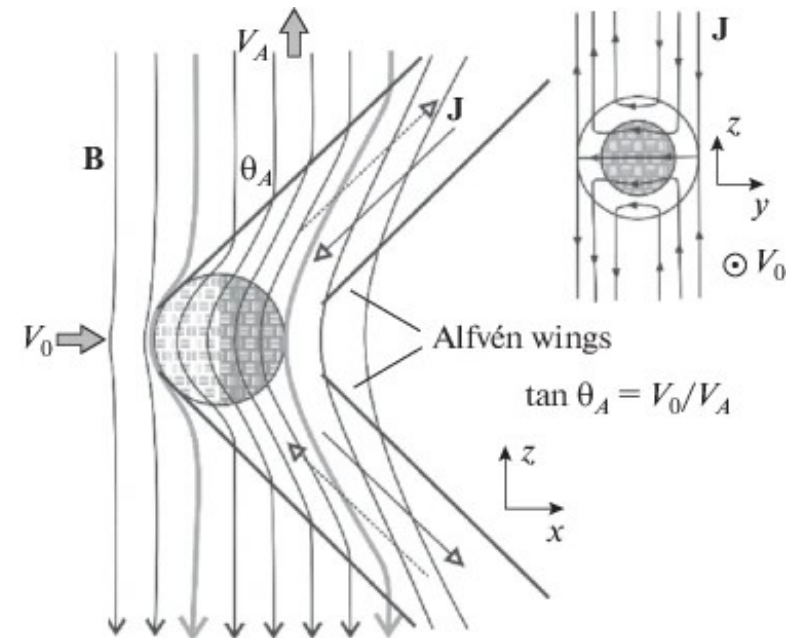
# Alfvén Wings

A plasma flow encountering an obstacle generates Alfvén waves that propagate along the magnetic field lines in the rest frame of the plasma. The plasma advects the magnetic field and the waves are simultaneously convected. As a result, the flow diverts around the object and forms two tubes on both sides of the obstacle (below and above). These tubes are known as the Alfvén wings and they can significantly alter the flow characteristics of the plasma.

The Alfvén wings point in the direction of the Alfvén characteristics ( $\mathbf{C}_A^\pm$ ) in the frame of the obstacle:

$$\mathbf{C}_A^\pm = \mathbf{v} \pm \frac{\mathbf{B}}{\sqrt{\rho\mu_0}} \quad (137)$$

(+) in the case of propagation toward the southern hemisphere and (-) toward the northern hemisphere of the object.



The Alfvén conductance controls the maximum current that can be carried by the Alfvén wave. It is (Neubauer 1980)

$$\Sigma_A = \frac{1}{\mu_0 V_A (1 + M_A^2 \pm 2M_A \sin \theta)^{1/2}} \quad (141)$$



# Relativistic Alfvén Wings (I)

Our equation:

$$\mathbf{C}'^s_A = \mathbf{v}' - \frac{\mathbf{B}'}{s\lambda}$$

$$\lambda = \left( \mu_0 \rho' + \frac{B'^2}{c^2} \right)^{1/2}$$

must be computed in the observer's frame  $R_o$ , since it will be used to derive the value of the electric current associated to the Alfvén wings. We write the velocity and the magnetic field as the sum of a longitudinal component that is parallel to  $\mathbf{v}_0$ , and a transverse vector component.

Let us transform the velocity of the fluid  $\mathbf{v}$  and the magnetic field  $\mathbf{B}$  to the wind's rest frame  $R_w$ , in special relativity they transform according to:

$$\mathbf{v}'_l = \frac{\mathbf{v}_l - \mathbf{v}_0}{1 - \frac{\mathbf{v}_0 \cdot \mathbf{v}}{c^2}}$$

$$\mathbf{v}'_t = \frac{\mathbf{v}_t / \gamma_0}{1 - \frac{\mathbf{v}_0 \cdot \mathbf{v}}{c^2}}$$

Where  $\gamma_0$  is the Lorentz factor of the unperturbed wind given by:

$$\gamma_0 = \left( 1 - \frac{v_0^2}{c^2} \right)^{-\frac{1}{2}}$$

## Current Carried by an Alfvén Wing

$$\nabla \cdot \mathbf{E} = \mu_0 \mathbf{j} \cdot \mathbf{U}_s$$

$$\mathbf{U}_s = \mathbf{v}_0 - \frac{s\mathbf{B}_0}{\gamma_0^2 \alpha}$$

Letting  $J_s$  be the projection of the current density along  $\mathbf{U}_s$ , we have:

$$\begin{aligned} \nabla \cdot \mathbf{E} &= \mu_0 \mathbf{j} \cdot \mathbf{U}_s \\ \nabla \cdot \mathbf{E} &= \mu_0 |\mathbf{j}| |\mathbf{U}_s| \cos \beta \\ \nabla \cdot \mathbf{E} &= \mu_0 J_s |\mathbf{U}_s| \end{aligned} \quad (211)$$

and defining  $\Sigma_A$ :

$$\begin{aligned} \Sigma_A &= \frac{1}{\mu_0 |\mathbf{U}_s|} \\ &= \frac{\alpha \gamma_0^2}{\mu_0 B_0} \frac{1}{\left( \frac{\alpha^2 \gamma_0^4 v_0^2}{B_0^2} - 2s \frac{\alpha \gamma_0^2 v_0}{B_0} \sin \theta + 1 \right)^{1/2}} \end{aligned}$$

$\gamma_0 \gg 1$  and  $c_A \gg c$ , that is relevant for a pulsar's wind:

$$\Sigma_A \approx \frac{1}{\mu_0 c}$$

## Relativistic Alfvén Wings (II)

Let the free parameter  $E_i$  be the electric field along the planet created by its ionosphere or surface internal resistance. At large distances from the wake, the electric field converges to the convection field  $\mathbf{E}_0$ . Neubauer gives useful expressions for the total current  $I$  flowing along an Alfvén wing. Letting the planet's radius be  $R_p$ , he obtains:

$$I = 4(E_0 - E_i)R_p\Sigma_A = 4\left(\frac{\Omega_*\Psi}{r} - E_i\right)R_p\Sigma_A \quad (217)$$

For the Joule dissipation power in the solid body,  $\dot{E}_J$ , which is the production of heat when an electric current pass through a conductor:

$$\dot{E}_J = 4\pi R_p^2 E_i(E_0 - E_i)\Sigma_A \quad (218)$$

The maximum Joule dissipation occurs when  $E_i = E_0/2$ ,

Considering  $E_i = E_0 \sim cB_\phi$

$$\frac{\dot{E}_J}{\pi R_p^2} \approx E_0^2 \Sigma_A \approx \frac{c^2 B_\phi^2}{\mu_0 c} = \frac{c B_\phi^2}{\mu_0} \quad (220)$$

so that the maximum power involved in an Alfvén wing is:

$$\dot{E}_J = \frac{\pi c R_b^2 (B_0^\phi)^2}{\mu_0} \quad (221)$$

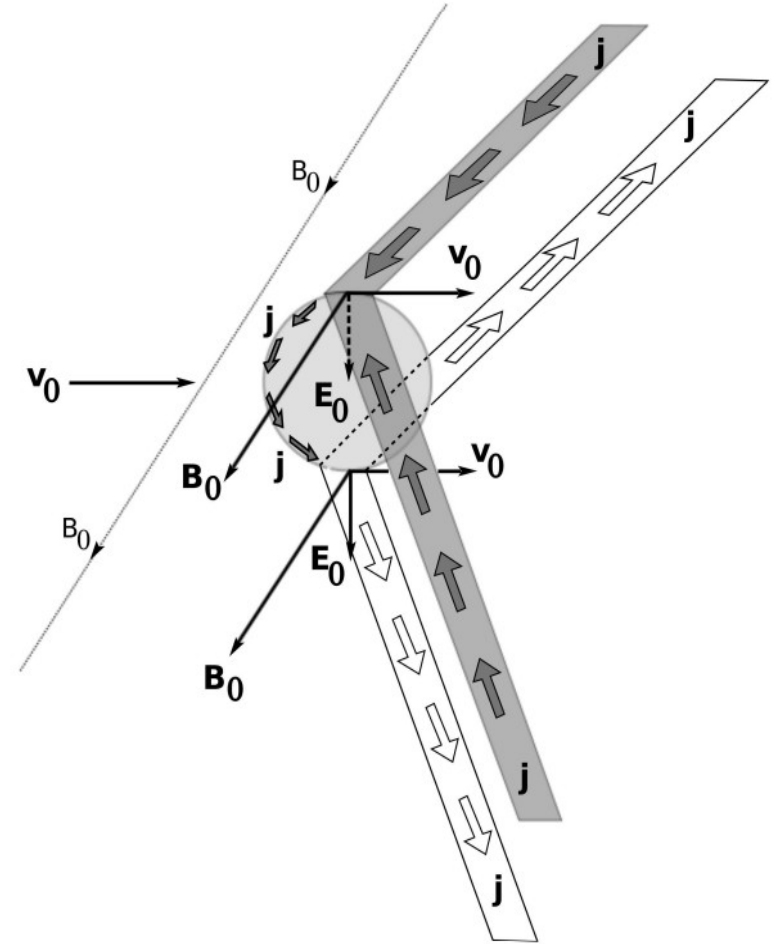


**Fig. 1.** Schematic view of a unipolar inductor.

## (4) Bode's Law

A generalized radio-magnetic Bode's law is derived. It relates the expected power-radiated of a magnetized flow-obstacle system ( $P_{rad}$ ) to the input power convected on the obstacle ( $P_{inp}$ ).

Depending on the various types of plasma flow-obstacle interactions, the input power is different in origin but its form will remain the same. Assuming a scaling law, it is expected:

$$P_{rad} \propto P_{inp}$$

It was found that in all cases the electromagnetic power ( $P_d$ ) dissipated is :

$$P_{rad} = \beta P_d$$

$$\beta = 2 \times 10^{-3}$$

The dissipated power is just a fraction of the magnitude of the Poynting vector convected on the cross-sectional area of the planet



## Density Flux

The maximum power involved in an Alfvén wing in function of the distance  $d$  and the radius  $R_{ob}$  is found by using equation:

$$\dot{E}_J = P_d = \frac{\pi}{\mu_0 c^3 r^2} R_{ob}^2 R_*^6 B_*^2 \Omega_*^4 \quad (262)$$

For a scaling law, it is expected:

$$P_{rad} = \beta_5 P_d \quad (263)$$

Hence, the maximum dissipated power in an Alfvén wing is:

$$P_{rad} = \beta_5 \frac{\pi}{\mu_0 c^3 r^2} R_{ob}^2 R_*^6 B_*^2 \Omega_*^4 \quad (264)$$

With  $2 \times 10^{-3} \leq \beta_5 \leq 10^{-2}$  (Zarka et al. [2001]; Zarka [2007])

The total average power radiated in the radio range of a magnetized flow-obstacle system can be calculated as:

$$P_{rad} = \Omega_A d^2 \int_{\omega_{min}}^{\omega_{max}} S(\omega) d\omega \quad (265)$$

Where  $S(\omega)$  is the radio flux density expected from a magnetized obstacle at a distance  $d$  from the source inside the solid angle  $\Omega_A$  of the beam of emitted radiation in the source frame, and  $[\omega_{min}, \omega_{max}]$  is the typical emission bandwidth. Assuming that  $S(\omega)$  is approximately constant over the emission bandwidth:

$$P_{rad} = \Omega_A d^2 S(\omega) \Delta\omega \quad (266)$$

$$S(\omega) = \frac{P_{rad}}{\Omega_A d^2 \Delta\omega} \quad (267)$$

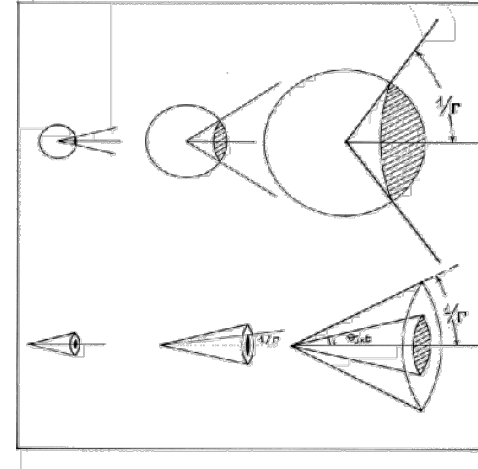
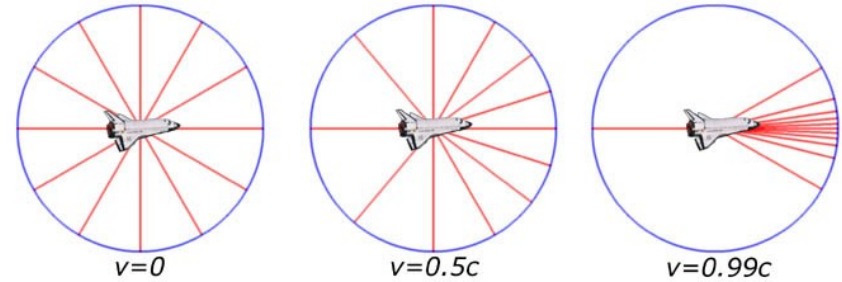
The average flux density in Jy of radio waves at distance  $d$  from the source inside the cone of emission is:

$$\left(\frac{\langle S \rangle}{\text{Jy}}\right) = 10^{-27} A_{\text{cone}} \left(\frac{\gamma_0}{10^5}\right)^2 \left(\frac{\beta_5}{10^{-3}}\right) \times \left(\frac{\dot{E}_J}{W}\right) \left(\frac{\text{Gpc}}{d}\right)^2 \left(\frac{1\text{GHz}}{\Delta\omega'}\right) \quad (284)$$

where  $\Delta\omega'$  represents the emission spectral bandwidth,  $\gamma_0$  is the Lorentz factor of the pulsar wind.  $A_{\text{cone}}$  is an anisotropy factor and is related to the solid angle  $\Omega_A$  by:

$$A_{\text{cone}} = \frac{4\pi}{\Omega_A} \quad (285)$$

In the source frame,  $A_{\text{cone}}$  takes the value of 1 if the radiation is isotropic, otherwise,  $A_{\text{cone}} > 1$ . In this case  $S = \langle S \rangle$ . The  $\gamma_0^2$  factor is a consequence of the relativistic beaming. When the Lorentz factor is much greater than 1 (i.e.,  $\gamma_0 \gg 1$ ), then the radio emissions are focused into a cone of characteristic angle  $\sim \gamma_0^{-1}$  (Mottez et al.



$$S(\omega) = \frac{P_{\text{rad}}}{\Omega_A d^2 \Delta\omega}$$

$$\left(\frac{\langle S \rangle}{\text{Jy}}\right) = 10^{-27} A_{\text{cone}} \left(\frac{\gamma_0}{10^5}\right)^2 \left(\frac{\beta_5}{10^{-3}}\right) \times \left(\frac{\dot{E}_J}{W}\right) \left(\frac{\text{Gpc}}{d}\right)^2 \left(\frac{1\text{GHz}}{\Delta\omega'}\right)$$

## (5) Compare predicted flux densities with simulated outcomes using PLUTO

The relativistic module of PLUTO can be used to obtain emission powers when the obstacle is conductive. The results can be compared with the predicted flux densities, using average parameters for the known pulsars characteristics.

	$\langle S_a \rangle$ (750) (mJy)	$\langle S_b \rangle$ (250) (mJy)	$\langle S_c \rangle$ (100) (mJy)	$\gamma$	$P_{rad}$ (W)	$B_0$ (G)	$\Delta\omega$ (MHz)	LOFAR (750)	MeerKAT (750)	SKA (750)
NEW	$4.8843 \times 10^3$	$4.3958 \times 10^4$	$2.7472 \times 10^5$	5.795	$1.05 \times 10^{20}$	3.6	10.08	YES	YES	YES
OLD	0.056488	0.50839	3.1774	2.0	$7.08 \times 10^{12}$	$2.5 \times 10^{-3}$	0.007	NO	NO	NO



# Summary

- Planets around pulsars are not very often,  $< 0.5\%$ , with a variety of possible kinds of evolution.
- Auroras are present in almost all planets in the Solar system.
- We try our tool for aurora on the pulsar planets, with relativistic module of PLUTO.
- Radio emission from pulsar planets could be visible even with current instruments, so we put a challenge to the observers. It would give us an additional window to study the pulsar wind.
- Artistic version of the results was showed in public almost 25 years before the scientific discussion.
- Planets as obstacles in the super-relativistic flow
- With the super-relativistic flow and complete integration, we repeat the challenge!